CHALMERS
UNIVERSITY OF TECHNOLOGY

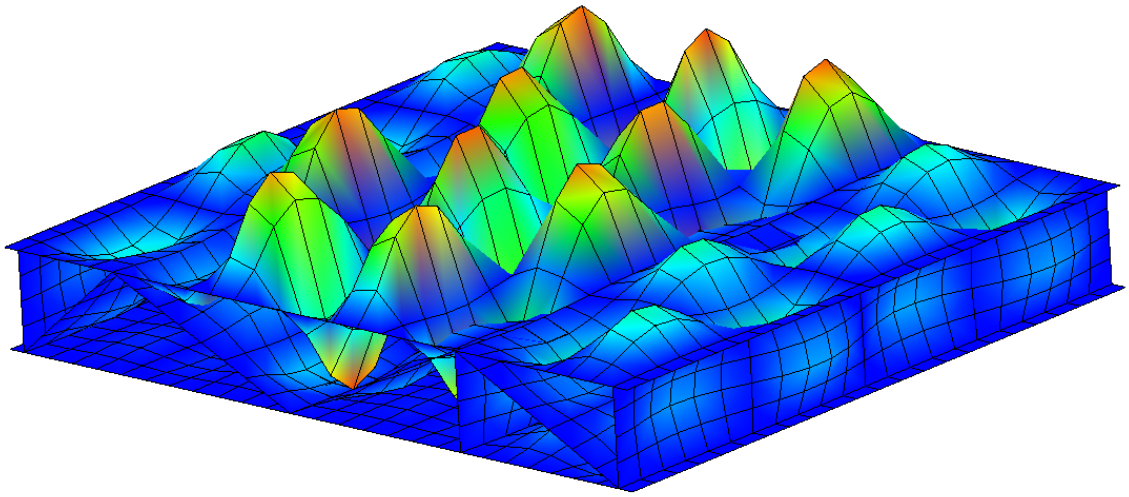

Optimization of Train Floors with Acoustic and Structural Constraints

Master's thesis in the Master's Programme Sound and Vibration

JOHAN WITTSTEN

Department of Civil and Environmental Engineering
CHALMERS UNIVERSITY OF TECHNOLOGY
Gothenburg, Sweden 2016

MASTER'S THESIS BOMX02-16-6

Optimization of Train Floors with Acoustic and Structural Constraints

Master's thesis in the Master's Programme Sound and Vibration

JOHAN WITTSTEN

Department of Civil and Environmental Engineering
Division of Applied Acoustics
CHALMERS UNIVERSITY OF TECHNOLOGY
Göteborg, Sweden 2016

Optimization of Train Floors with Acoustic and Structural Constraints
Master's thesis in the Master's Programme Sound and Vibration
JOHAN WITTSTEN

Examensarbete / Institutionen för bygg- och miljöteknik,
Chalmers tekniska högskola BOMX02-16-6

Department of Civil and Environmental Engineering
Division of Applied Acoustics
Chalmers University of Technology
SE-412 96 Göteborg
Sweden
Telephone: + 46 (0)31-772 1000

Cover:
Modal pattern of a structural floor made out of extruded panels. Plot obtained in analysis using VA-One, ESI Group (2015).

Name of the printers
Göteborg, Sweden 2016

Optimization of Train Floors with Acoustic and Structural Constraints

Master's thesis in the Master's Programme Sound and Vibration
JOHAN WITTSTEN
Department of Civil and Environmental Engineering
Division of Applied Acoustics
Chalmers University of Technology

ABSTRACT

For operating trains substantial noise levels are generated in the bogie from wheel-rail contact and for higher speeds also from aero-acoustic sources. Train manufacturers wish to minimize the transmission to the interior, for example by applying damping layers in the floor construction or by other design measures. Such measures typically implies added mass. When designing noise control measures, the goal is to achieve the necessary sound reduction needed at lowest possible mass per unit area.

This thesis consists of two parts. The first part aims at evaluating transmission models for analysis of air-borne sound transmitted through double walls, which can be considered a simplified description of a typical train floor. Double wall models were developed in two different acoustic software, one using Statistical Energy Analysis (SEA) and the other using Transfer Matrix Methodology (TMM). Transmission loss (TL) results from both models are compared with existing measurement data. Based on the two models, parameter studies regarding the filling ratio of the cavity and the flow resistivity of the filling material were made. Both SEA and TMM models agreed well with the measurement data when having a partly filled cavity. The case with an empty cavity was more problematic. The results also showed good agreement when changing the air-flow resistivity.

In the second part an optimization routine to minimize the floor mass is applied. Constraints were defined on maximum allowed floor deflection and interior sound level. A structural floor of extruded panels was addressed. For computational speed a concept was applied for which an FE model of a periodic cell of the structure is analyzed using periodic boundary conditions. FE calculation results are post-processed to determine acoustic transmission loss and an analytic beam model for the deflection is applied. A MATLAB script was written to control the optimization with panel thicknesses and cell dimensions taken as design variables. The script applies geometric changes to an SEA model, which for each new iteration is re-meshed into a new FE model.

Solutions that fulfills the specified constraints with the smallest mass are sought. Using an original floor structure with mass per unit area 23.8 kg/m^2 as reference, the optimization results in a final design with 18.0 kg/m^2. Convergence from different starting points is verified.

Keywords: Double walls, Statistical Energy Analysis, Transfer Matrix Methodology, Structural optimization, Mass minimization, Sandwich

Contents

Acknowledgements

This thesis was written as part of the Master's Programme in Sound and Vibration at Chalmers University of Technology.

When choosing a topic for my thesis, I wanted something that was both challenging and interesting. Luckily that was exactly what I found. Working with this thesis was a great experience and I am happy that I had the opportunity to do so. This has been the most challenging project I have ever laid my hands on. Thanks to a lot of great people around me, I can now happily say that I am finished. That last word means the most to me.

My warmest thanks goes to all the great individuals that have helped me along the way. I have learned a lot over this last year. When things become difficult, it matters the most to have friends around. The process of writing this thesis has been very rewarding. One of my favorite comedians, Mitch Hedberg, said in one of his jokes:

"An escalator can never break: it can only become stairs. You should never see an 'Escalator Temporarily Out of Order' sign, just 'Escalator Temporarily Stairs'. Sorry for the convenience."

I would like to thank the entire Acoustics and Vibration group at Bombardier Transportation and my supervisor Ulf Orrenius for proposing the thesis subject. Thank you all for welcoming me to the office in Västerås and also for finding a place for me to stay while writing the thesis.

When working with my computer models, I was very lucky to have the great support of the ESI Group. Thank you for taking the time to answer all my questions, I could not have made it without your help.

Thank you Patrik Höstmad and Carsten Hoever at Applied Acoustics for your encouraging help and supervision.

Most of all, I would like to thank Matilda.

Göteborg, April 2016
Johan Wittsten

1 Introduction

1.1 Background

For operating trains substantial noise levels are generated in the bogie from wheel-rail contact and for higher speeds also from aero-acoustic sources. Train manufacturers wish to minimize the transmission to the interior, for example by applying damping layers in the floor construction or by other design measures. Such measures typically imply added mass. When designing noise control measures, the goal is to achieve the necessary sound reduction needed at lowest possible mass per unit area.

1.2 Problem description

This thesis is divided into two parts.

The first part focuses on developing validated transmission models for analysis of air-borne sound transmitted through a double wall, which can be seen as a simplified description of a train floor. A typical train floor is as a three-layered structure, seen in Figure 1.1, with an inner floor and a structural floor separated by a cavity with dampers and foam. This structure has essentially the same elements as a double wall.

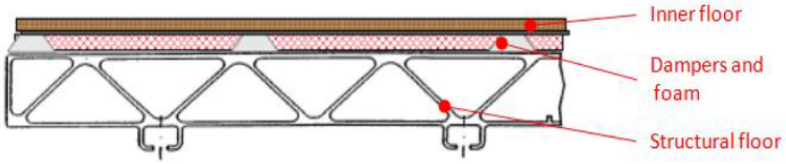

Figure 1.1: Typical setup of a train floor

The second part investigates the possibility to solve a structural optimization of a train floor with constraints on both structural and acoustical performance. When in motion, train wheels generate noise, which will be transported through the train floor and walls to the inside of the train car. A common design measure for train manufacturers is to minimize the internal noise levels, for example with a damping layer in the floor construction. This however often implies added mass. When designing noise control measures, the goal is to achieve the best possible sound reduction without exceeding the maximum weight allowed. This thesis aims at minimizing the mass of a train floor, while fulfilling constraints regarding maximum deflection and interior sound pressure level inside the train car.

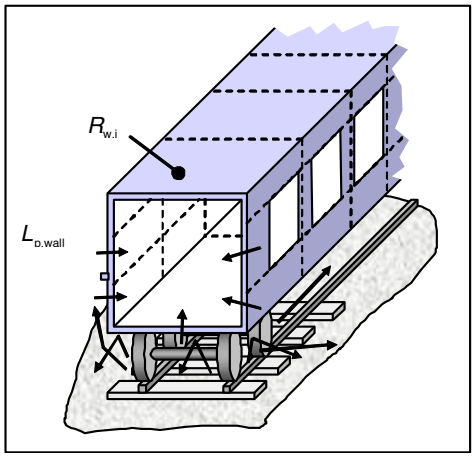

Figure 1.2: Train car with sound transmission paths

1.3 Aim

- Develop validated transmission models for analysis of air-borne sound through train floors.
- Apply an optimization routine for floor mass minimization with the sound transmission properties as a constraint together with deflection requirements.

1.4 Limitations

This thesis aims at solving an optimization problem on how to minimize mass on a train floor, but is not aiming at finding an optimal design solution for commercial use. The main task of the optimization is rather to show the possibility to combine constraints from different disciplines in the design process.

1.5 Method

A literature review is conducted to better understand the topics covered in this thesis. Focus is set to evaluate existing measurement data of double walls, and to examine previously made optimizations of lightweight structures.

The next step is to create acoustic models of double walls using Statistical Energy Analysis (SEA) and Transfer Matrix Methodology (TMM) and benchmark with measurement data.

The final task is to create a computer script to run a mass minimization routine on a structural floor typical for trains with constraints on maximum static deflection and maximum interior sound levels.

2 Theory

2.1 Wave propagation

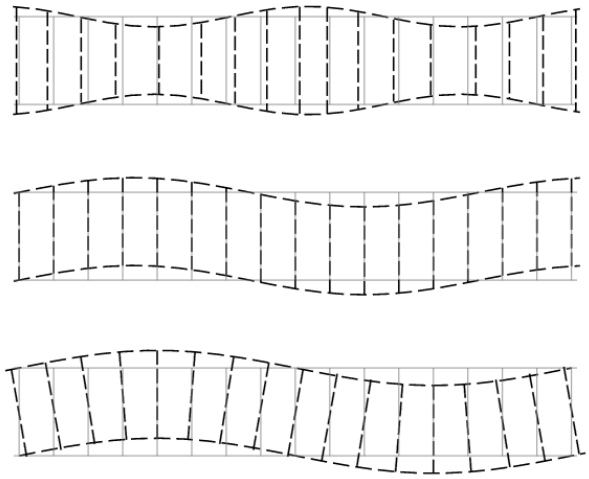

Figure 2.1: Wave types common in plates. Top: Longitudinal wave. Middle: Transverse wave. Bottom: Bending wave.

A plate can basically contain three different types of waves; bending waves, longitudinal waves, and transverse (shearing) waves. Bending waves are of special interest when considering sound radiation. When a plate radiates sound it can be interpreted as if the moving structure is putting a load onto the connecting fluid medium, which causes the particles in the fluid to move, and lets energy travel as propagating sound. Bending waves have particle motion in the normal direction of the plate, which is what causes the loading of the fluid. Similarly, when a sound field is impinging on the plate, bending waves are the only ones that can arise (Craik, 1996).

A distinction is made between the speed at which energy is transported (c_g: group velocity) and the speed at which deformations are propagated (c_B: phase velocity). Here lies a differentiation between the wave types; the group and phase velocities are equal when considering longitudinal and transverse waves, however the situation is different for bending waves as the group velocity is equal to twice the phase velocity on thin plates (Craik, 1996),

$$c_g = 2c_B \qquad (1)$$

2.2 Transmission of sound

This section will describe common attributes of sound transmission.

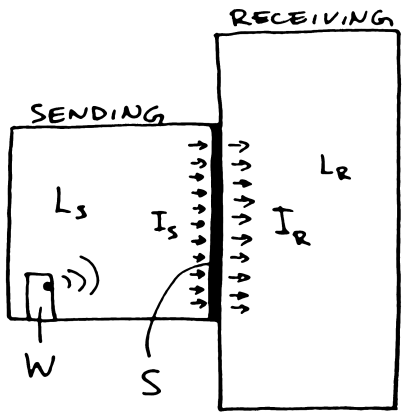

Figure 2.2: Concept of sound transmission

Consider two rooms separated by a wall, where one of the rooms contains a noise source. How much sound that travels through the wall is determined by the transmission coefficient τ,

$$\tau = \frac{W_R}{W_S} \tag{2}$$

where W_R is the power of the transmitted sound and W_S is the incident sound power. The definition of acoustical power is stated as,

$$W = \frac{1}{2}\Re\{\bar{p}v\} = \frac{|p|^2}{2}\Re\left\{\frac{1}{Z_c}\right\} \tag{3}$$

where p is the complex acoustic pressure amplitude and $\bar{p}$ is the pressure complex conjugate, v is the complex particle velocity amplitude, and $Z_c = p/v$ denotes the characteristic impedance of the medium. Because the wall has the same medium on both sides (air) it is possible, assuming same wave type on either side, to express the transmission coefficient τ as,

$$\tau = \left|\frac{p_R}{p_S}\right|^2 \tag{4}$$

It is possible to express the power in terms of sound intensity $I = \tilde{p}^2/4\rho_0 c_0$ with ρ_0 defined as the density of air and c_0 as the speed of sound in air, assuming that the two rooms separated by the wall as in Figure 2.2 both contain a diffuse field. The acoustic power incident on the wall can be written as,

$$W_S = I_S S \tag{5}$$

Where I_S is the incident sound intensity and S is the surface area of the separating wall. This leads to the following expression for the incident power,

$$W_S = \frac{\tilde{p}_S^2}{4\rho_0 c_0} S \tag{6}$$

The transmitted power can be calculated analogously with A_R denoting the absorption area of the receiving room,

$$W_R = \frac{\tilde{p}_R^2}{4\rho_0 c_0} A_R \tag{7}$$

This makes it possible to write the transmission coefficient as,

$$\tau = \frac{\tilde{p}_R^2}{\tilde{p}_S^2} \frac{A_R}{S} \tag{8}$$

The transmission coefficient is needed when calculating the transmission loss R,

$$R = 10 \log_{10} \frac{1}{\tau} \tag{9}$$

Some authors prefer to call R the sound reduction index, however this report will use the term transmission loss (TL). Equation (9) combined with equation (8) can be rewritten with the help of logarithmic rules, leading to the following expression,

$$R = L_S - L_R + 10 \log_{10} \frac{S}{A_R} \tag{10}$$

where L_S is the sound pressure level in the sender room and L_R is the sound pressure level in the receiving room. This means that the transmission loss is easily calculated as the difference in sound pressure levels between the two rooms with an additional term that accounts for the absorption inside the receiving room.

2.2.1 Single wall

A plate of infinite size, subject to vibrations, excites the air depending on coupling between the bending waves in the plate and the longitudinal waves in the air. What determines the coupling between two connecting media is the relation between wavelengths as illustrated in Figure 2.3, showing the wavelength in a plate λ_B and the corresponding wavelength of the connecting air λ_{air} as sound is radiating from the plate at angle θ.

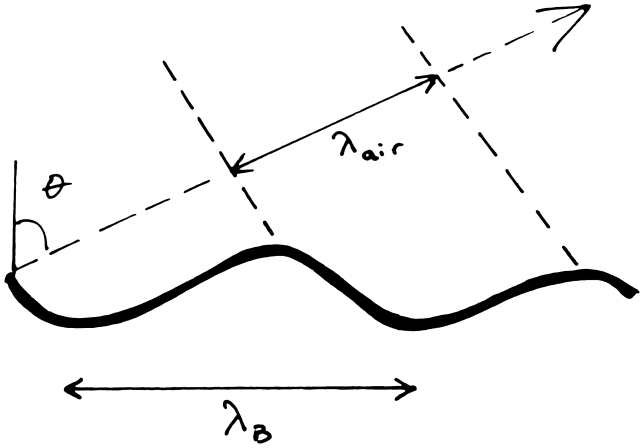

Figure 2.3: Coupling plate and air determined by the relation between wavelengths.

Coupling between the two media occurs if the wavelength in air fits the wavelength of the plate. This happens at $\lambda_B > \lambda_{air}$ and is the only case when the air will be excited with free vibrations. What happens at $\lambda_B = \lambda_{air}$ where the plate and air share the same wavelength is a complete resonant transmission, commonly known as the critical frequency. Below the critical frequency the wavelength in air is larger than the wavelength in the plate, and the plate only experiences non-resonant transmission. This means that incident waves in air cannot couple with the wave pattern in the plate, and the air experiences the plate as a single mass object that can only be excited with forced vibrations.

What happens at $\lambda_B < \lambda_{air}$ when no sound radiates is called a hydrodynamic short-circuiting, which is the near-field effect of air moving back and forth between local displacements as the plate vibrates. Hydrodynamic short-circuiting is especially related to plates of infinite size. However, finite plates can also experience this effect, although only for higher frequencies. A finite plate still radiates because the hydrodynamic short-circuiting cannot successfully cancel out the air movement at the plate edges. Figure 2.4 illustrates the effect for different frequencies.

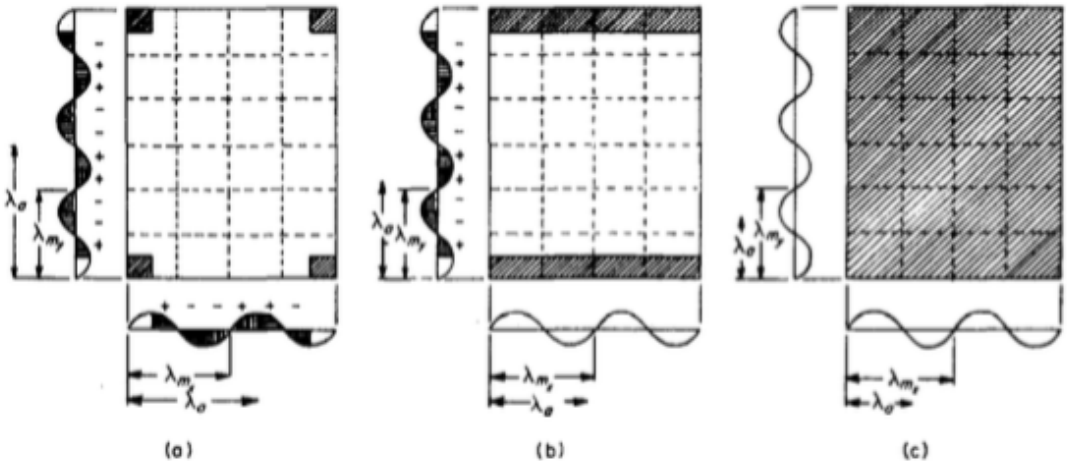

Figure 2.4: Radiation at plate edges (Fahy, 1985).

2.2.2 Double wall

A double wall is made of two plates separated by a cavity. Assuming diffuse field on both sides of the wall and inside the cavity and applying Equation (10) to the two plates of the double wall, Tageman (2013) derives the following equation:

$$R_{dw} = R_{plate1} + R_{plate2} + 10\log_{10}\frac{A_{cavity}}{S} \qquad (11)$$

This expression tells that the transmission loss of the double wall depends on the reduction indices of the two separate plates with the additional term regarding the cavity damping. Equation (11) is valid when $f \gg f_0$ and when no short-circuiting is present.

Sound is transmitted over the plates by either resonant or non-resonant transmission. Under the critical frequency, the double wall acts as a mass-spring system where the cavity works as a spring on the two plate masses. The mass-spring system has its lowest resonance at

$$f_0 = \frac{1}{2\pi}\sqrt{\frac{\rho_0 c_0^2}{d}\cdot\frac{m_1'' + m_2''}{m_1'' m_2''}} \qquad (12)$$

where m_1'' and m_2'' are the masses of the two respective plates and d is the separating distance between them. Below this frequency, the double wall behaves like a single plate with the combined mass of the double wall plates. Resonances inside the double wall leads to a decreased sound reduction, which can be made less prominent by having plates with different masses (Fahy, 1985).

Most of the transmission below the critical frequency is due to non-resonant transmission. If the cavity depth is small, there may also be non-resonant coupling between the two plates (Craik, 1996).

In practical applications the transmission is at higher frequencies determined by "short circuiting" of energy through connecting elements (Craik, 1996). This phenomenon will be illustrated by experimental and calculation examples in Section 3.4.

2.3 Transfer Matrix Methodology

2.3.1 Principles of TMM

Transfer Matrix Methodology (TMM) builds around sound waves being propagated through constructions made out of a number of different layers with specified thicknesses and material properties (Allard & Atalla, 2009). Figure 2.5 shows a typical TMM application of a single layer construction.

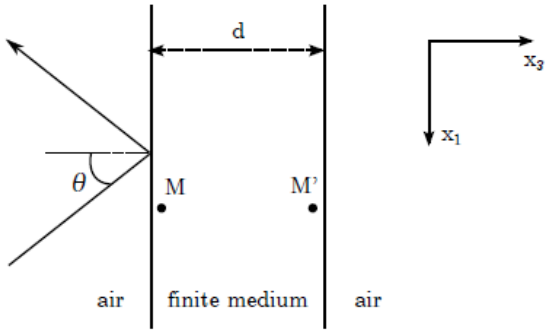

Figure 2.5: Example of TMM layer (Tageman, 2013)

When using TMM the material layers are considered to be infinite in x_1 and x_2 directions. An incident sound wave hits the material with an angle θ and causes a wave field that propagates inside the finite dimension of the layer. The properties of each layer is described by a transfer matrix that relates the pressure and particle velocity on both sides of the layer, such that

$$\begin{bmatrix} p(M) \\ v_3(M) \end{bmatrix} = \begin{bmatrix} T_{11} & T_{12} \\ T_{21} & T_{22} \end{bmatrix} \begin{bmatrix} p(M') \\ v_3(M') \end{bmatrix} \qquad (13)$$

This approach makes it possible to calculate sound transmission of a multi-layered construction as a multiplication of several different transfer matrices.
The transfer matrix of a double wall with a cavity containing an absorber would be calculated as:

$$T_{total} = T_{plate1} \cdot T_{cavity\ fluid} \cdot T_{cavity\ absorber} \cdot T_{plate2} \qquad (14)$$

When considering typical multilayered constructions, the layers usually have different properties due to the inherent physical differences in materials. TMM can be applied to describe many materials, such as fluid, visco-elastic, poro-elastic and solid media. Details on these material descriptions have been presented by Tageman (2013) and Orrenius et al (2010).

2.3.2 Limitations of TMM

A few problems arise when constructing a mathematical representation of a double wall with the Transfer Matrix Methodology. Because each layer (plate, filling material, air) is infinitely large in all directions other than the cross-section, the model is not able to represent resonances that would normally occur in a real double wall partition. These resonances stem either from standing waves inside the wall cavity, or when the two plates interact with each other as the intermediate air cavity works as a spring.

Another problem is regarding the transmission of waves in double walls. If considering the incoming sound as a field of obliquely incident plane waves, the reflected waves within the wall will co-align with the transmitted waves and cause positive interference (Grosveld, 1985). This is a problem for double walls of infinite size and will exaggerate the transmission of sound through the structure, as illustrated in Figure 2.6. This also occurs for double walls of finite size, but is more complex due to edge effects. However, the practical limitations of positive interference are mainly attributed to double walls with empty cavities.

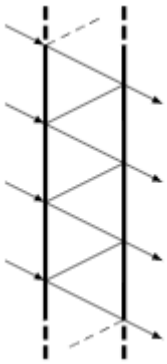

Figure 2.6: Transmission of sound through a double wall of infinite size causing positive interference (Grosveld, 1985)

Because these are well known limitations, researchers have tried different methods to improve TMM modeling. A commonly used method to account for the finite size of elements is to apply a spatial windowing technique. The spatial windowing method deals with the diffraction due to a finite opening, but not with the effects of resonances in panels and in cavities. An infinite plate exposed to a sound field containing only one frequency can be considered as being excited by one wave number carrying the entire energy. This is illustrated in Figure 2.7.

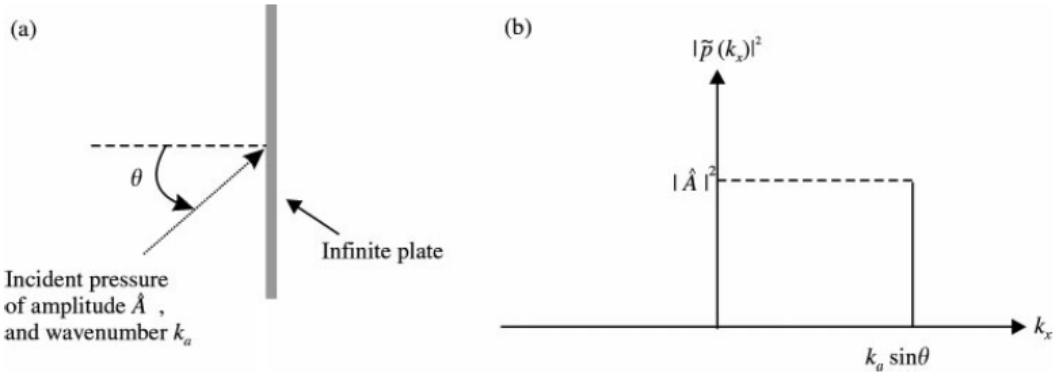

Figure 2.7: (a) Infinite plate subject to impinging wave field. (b) Associated wavenumber spectrum (Villot, 2001)

When using the spatial windowing technique, the sound field is modified to let energy excite the plate over the entire wave number spectrum. This method was first introduced by Villot (2001) and is a good way to improve predicted results by incorporating diffraction of incident sound, which would normally occur at the plate edges for finite sized structures. Figure 2.8 illustrates the effect of the spatial window.

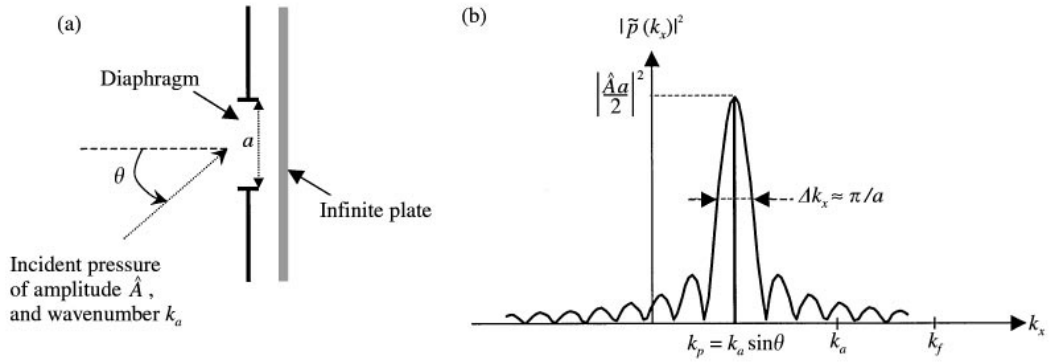

Figure 2.8: (a) Applying a spatial window. (b) Associated wavenumber spectrum (Villot, 2001)

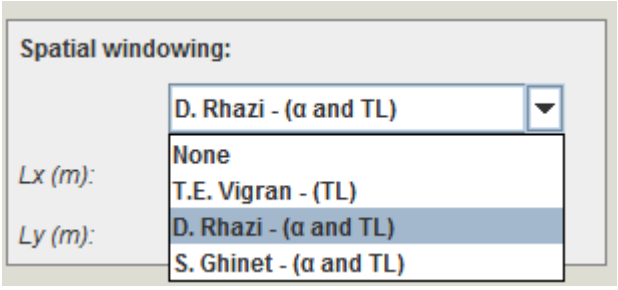

Figure 2.9: Setting in AlphaCell for choosing spatial windowing algorithm

2.4 Statistical Energy Analysis

Statistical energy analysis (SEA) has been a valuable engineering tool for vibro-acoustic problems for many years and has been thoroughly examined by authors like Lyon (1995) and Craik (1996). SEA can be applied in the design process to predict the response of complex structures when subject to external forces and to identify critical parts of structures that carry large amounts of energy. This chapter will serve as a brief introduction to SEA, pinpointing some of the key principles of SEA that are valuable for this thesis.

2.4.1 Principles of SEA

Statistical energy analysis is a methodology for calculating the dynamical energy in complex structures that can be applied when for instance calculating transmission loss of double walls. A SEA model consists of a number of smaller interconnected subsystems that together form a representation of the larger system. SEA theory is based on the notion that the response of a subsystem entirely depends on the resonances in the subsystem, and thus is proportional to the damping (Craik, 1996). One or more subsystems receive energy input from external sources. Energy is then transported within the system between coupled subsystems or dissipated because of damping. Each subsystem relies on a power balance based on the conservation of energy within the entire system. The rate of dissipated energy of a subsystem is assumed proportional to the energy in the subsystem, and the power flow between two subsystems is assumed to be directly proportional to the difference in their modal energies. This means that when two coupled subsystems have the same energy per mode, the power flow is zero. Because the theory relies on resonances within every subsystem in order to properly predict the system response, SEA is often referred to as a high frequency method (Craik, 1996) (Barbagallo, 2013).

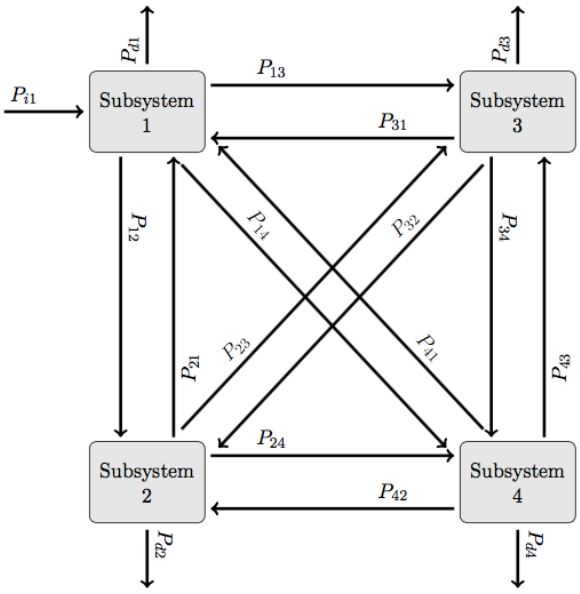

Figure 2.10: Example of a SEA system model

Figure 2.10 illustrates a generic SEA model in which P_{ij} is the input power of subsystem j, P_{dj} is the dissipated power of subsystem j and P_{jk} is the power flowing from subsystem j to k. When writing out the definitions of the parameters it is clear that they are very similar:

$$P_{dj} = \omega \eta_{dj} E_j \tag{15}$$

$$P_{jk} = \omega \eta_{jk} E_j \tag{16}$$

What separates them are the different loss factors, used in the definitions, where η_{dj} is the damping loss factor (DLF) and η_{jk} is the coupling loss factor (CLF). The DLF determines how much energy is dissipated from a subsystem as a result of material damping, damping from joints or acoustic radiation. The CLF is a central parameter in SEA theory that relates the average power flow between two coupled subsystems to be proportional to their difference in modal energies (Lyon, 1995).

The complete power balance of the system in Figure 2.10 can be written as:

$$P_{i1} + P_{21} + P_{31} + P_{41} = P_{d1} + P_{12} + P_{13} + P_{14} \tag{17}$$

$$P_{12} + P_{32} + P_{42} = P_{d2} + P_{21} + P_{23} + P_{24} \tag{18}$$

$$P_{13} + P_{23} + P_{43} = P_{d3} + P_{31} + P_{32} + P_{34} \tag{19}$$

$$P_{14} + P_{24} + P_{34} = P_{d4} + P_{41} + P_{42} + P_{43} \tag{20}$$

2.4.2 Limitations of SEA

SEA theory relies on a statistical framework particularly well suited for high frequencies, given that it requires each subsystem to contain a certain number of modes in the frequency band analyzed for the theory to be applicable. The number of modes is important because it dictates the possible amount of resonant modes that can transmit energy in a subsystem. If the number of modes in a subsystem is too small, estimations on the damping will be uncertain. The calculation certainty of the SEA model can be estimated from the modal overlap factor M, which is defined as the modal bandwidth divided by the average frequency spacing of modes. A lower limit for where SEA theory no longer applies can be taken as $M = 1$. Above this limit there will still be erroneous results, but the size of the errors will decrease with increasing frequency.

2.5 Optimization theory

2.5.1 Definitions

When working with optimization it is important to use the correct terminology. Presented in Table 2.1 are three important terms and their definitions. They will be used throughout the rest of the thesis.

Table 2.1 Definitions of common terms in optimization.

Objective function	A mathematical equation that can either be maximized or minimized with respect to a set of parameters and constraints.
Parameters	Function variables that can be changed during the optimization, usually within upper and lower bounds.
Constraints	Requirements that need to be fulfilled when minimizing or maximizing the objective function

As is stated in Table 2.1 the *objective function* is the actual goal of the optimization, typically either maximizing or minimizing a function that determines an important property such as mass, price or time. To achieve this goal, a given number of *parameters* need to be able to change in order to find the optimal solution. Lastly, an optimization task often has one or more *constraints* that need to be fulfilled when searching for a solution. The constraints can for example be specified from production requirements or design specifications.

2.5.2 Literary review on optimization

Previous work has been made within the topic optimization of structures with constraints on acoustic performance by several authors.

Wennhage conducted a mass minimization of a sandwich panel structure. Structural constraints were based on maximum stress and deflection, and an acoustic constraint was based on transmission loss of the structure (Wennhage, 2002). The paper discusses optimization theory, and says that optimization of sandwich panels with structural constraints has been a common subject for many years. It describes the challenges of designing a light weight structure that combines both high stiffness and damping of sound. The optimization was made with the Method of Moving Asymptotes (MMA) which was commonly used for optimization with structural constraints (Wennhage, 2002). Solving the optimization resulted in an optimized structure, which later was manufactured and compared to an original structure by measuring their respective airborne transmission loss.

Bartolozzi et. al. (2012a, 2012b) performed an optimization on a sandwich-based inner floor of a train car to minimize the mass, with acoustic constraint set on the weighted transmission loss. A structural constraint was set based on maximum deflection from distributed and point loads. Design parameters were defined as the different layer thicknesses of the structure. The authors used different methods of solving the optimization, evaluating the strengths of the methods and comparing their results with focus on the computational effort needed. The papers discuss the time consuming process that normally occurs when creating a structure that fulfills several different functional requirements, e.g. acoustic, thermal and mechanical. Normally each of these requirements are addressed individually. A great value of multidisciplinary optimization is the ability to cut time in the draft process when designing new structures. However, working with optimization becomes difficult when searching for mathematical representations that directly translates the physics of all specified requirements.

The evaluated methods in the paper by Bartolozzi (2012b) were divided in two groups; Gradient Based (GB) and Non-Gradient-Based (Non-GB) methods. Generally, GB methods require fewer iterations than Non-GB methods. GB methods on their own only guarantee local minimum convergence, however it is possible to find global minima solutions by solving the optimization routine from different starting points. The evaluated GB method was the Active-Set method, which is part of the `fmincon` MATLAB command. Active-Set applies a so called sequential quadratic programming (SQP) algorithm, solving a quadratic programming (QP) subtask every iteration. A complete explanation of the SQP algorithm is described by Arora (2004).

2.5.3 A short optimization example

Optimization aims at finding the best possible solution for a given problem, given some limiting criteria. Figure 2.11 shows a setup of an optimization problem where the objective is to minimize the volume of a cylinder shell.

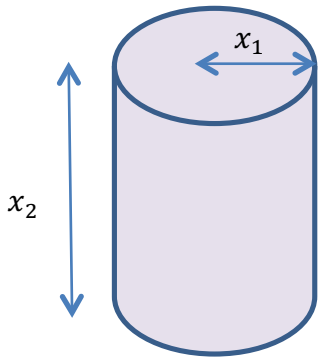

Figure 2.11: Cylinder optimization example

In this case, the objective function can be written as,

$$\min f(x) = \pi {x_1}^2 x_2 \qquad (21)$$

where the radius x_1 and height x_2 are the input parameters in millimeters. The parameters can be set to any number between the lower and upper bounds, as shown below

$$\begin{aligned} 30 < x_1 < 50 \\ 70 < x_2 < 90 \end{aligned} \qquad (22)$$

The problem has a mathematical constraint, relating the height and the radius of the cylinder as,

$$0 \leq -2x_1 + x_2 \leq 5 \qquad (23)$$

This simple example can be solved in MATLAB with the `fmincon` command

```
[x,fval] = fmincon(fun,x0,A,b,Aeq,beq,lb,ub)
```

where
`fun` is the objective function evaluated at x.
`x0` is the initial point at which the objective function is evaluated
`A, b` are matrices for linear inequality constraints $Ax \leq b$
`Aeq, beq` are matrices for linear equality constraints $A_{eq}x = b_{eq}$
`lb, ub` are vectors for lower and upper bounds
`x` is the solution, returned as an output from the function
`fval` is the value of the objective function at the solution

From Equation (23), the linear inequality constraints can be rewritten as,

$$\begin{aligned} 2x_1 - x_2 &\leq 0 \\ -2x_1 + x_2 &\leq 5 \end{aligned} \tag{24}$$

Which leads to the following MATLAB expressions,

```
>> A = [2 -1;-2 1];
>> b = [0;5];
>> Aeq = []; beq = [];
>> lb = [30;70];
>> ub = [50;90];
>> [x,fval] = fmincon(fun,x0,A,b,Aeq,beq,lb,ub)

x =
   32.5000
   70.0000

fval =
   2.3216e+05
```

The function `fmincon` solves a minimization problem over a series of iterations. It starts with an evaluation of the objective function `fun` at the initial point `x0`, and then proceeds with the several other objective function evaluations at different points close to `x0` in order to find the gradient. After having calculated the gradient at `x0`, the function sets a new point `x1` at which a new series of objective function evaluations begins in order to find the gradient at `x1`. This iterative process is repeated multiple times until the function converges to the point `xn` at which a minimum to the objective function has been found.

Following this example, the same principles can be used on the optimization problem this thesis aims at solving. The task is to minimize the mass per area of a structural floor, typical for train cars, such that requirements are met regarding the deflection from static loads and also regarding the A-weighted sound pressure levels inside the train car as an effect of sound being transmitted through the structural floor. Figure 2.12 illustrates the structure analyzed.

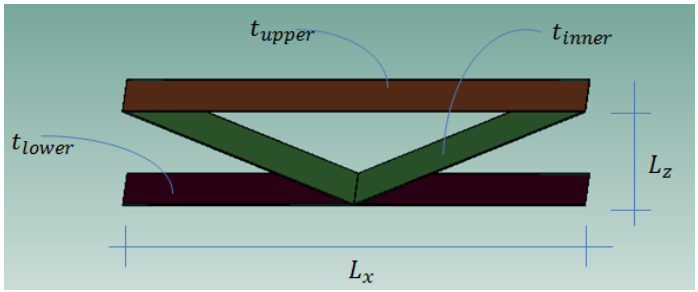

Figure 2.12: The analyzed structure with five parameters.

This is a complex optimization problem with nonlinear constraints. It is possible to solve with the same MATLAB `fmincon` command by adding the nonlinear constraints as a separate argument `nonlcon,` which tells the optimizer to analyze the structure with respect to a set of specified nonlinear constraints.

```
x = fmincon(fun, x0, [], [], [], [], lb, ub, nonlcon)
```

This choice of formulating the problem around mass minimization is due to that the weight is typically a cost driver in vehicle design projects, whereas noise levels and stiffness are stipulated by limiting design requirements. Alternatively, instead of minimizing the mass, one could minimize the transmitted sound power or the deflection and let the mass be one of the constraints.

3 Double wall modeling

The first part of this project comprises a study on double walls, with the aim to calculate the transmission loss for a double wall construction and compare the predictions with measured results from Hongisto et. al. (2002). The wall chosen to be modeled in this chapter, illustrated in Figure 3.1, is composed of two 2 mm steel plates separated by a partially filled cavity of depth d = 125 mm. Results from a similar study, but with cavity depth d = 25 mm, is presented in Appendix A.

The setup is modeled and validated as two separate studies; one on the effect of changing the amount of filling material inside the cavity, and one about changing the air-flow resistivity of the filling material.

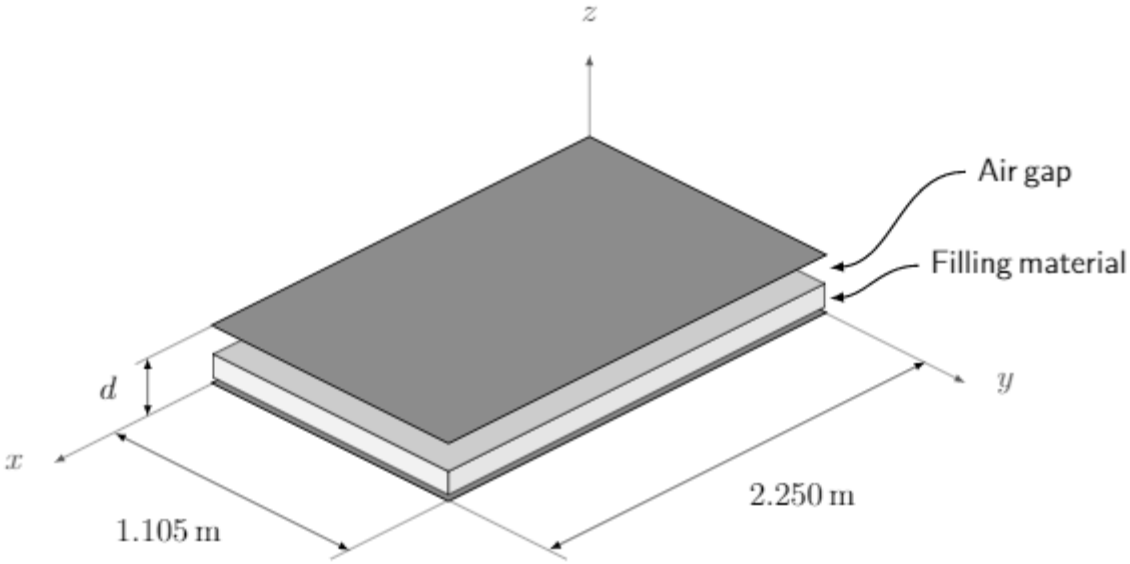

Figure 3.1: Two steel plates enclosing a partially filled cavity of depth d

Models of the wall were developed in the acoustic software VA-One and AlphaCell. The programs employ two different methodologies in their calculations; VA-One is using Statistical Energy Analysis (SEA) (Craik, 1996) and AlphaCell is based on the Transfer-Matrix Method (TMM) (Allard & Atalla, 2009). This makes the study an evaluation of not only the physics of the double wall construction, but also a comparison of the underlying calculation methodologies in the two software applied.

3.1 Material data

All input data necessary for creating the SEA and TMM double wall models are presented in Table 3.1.

Table 3.1: Input data for the VA-One and AlphaCell double wall models. Estimated values are marked with an asterix.

Material	Material property	Value	Model
Steel plates	Thickness [m]	0.002	SEA & TMM
	Poisson's ratio [-]	0.28	SEA & TMM
	Young's modulus [GPa]	200	SEA & TMM
	Density [kg/m^3]	7800	SEA & TMM
	Loss factor [-]	From (Hongisto, 2002)	SEA & TMM
Filling material	Flow resistivity [kPas/m^2]	8; 30	SEA & TMM
	Density [kg/m^3]	17; 61	SEA & TMM
Cavity	Hydraulic radius [m]	0.1	TMM
	Average absorption [%]	1*	SEA

It needs to be noted that the air cavity is described differently in the two programs. AlphaCell handles air cavities as porous media, and lets the user define a hydraulic radius (Allard & Atalla, 2009) of a fluid to account for viscous dissipation at an interface between air and a structure. The AlphaCell calculations are derived from (Allard & Atalla, 2009), and compute the viscous boundary layer from that of a cylindrical tube with radius R. For double walls they recommend to compute R so that it equals the static flow resistivity of a slit, however this approximation is only valid for low frequencies.

VA-One handles the damping of empty cavities by either assigning a loss factor for the enclosed air, or by assigning an average absorption to the panels surrounding the cavity. The effect of absorption material in a cavity is modelled by assigning one or multiple layers of filling material to the enclosing surfaces surrounding the cavity. The absorptive properties are determined by the flow resistivity and density of the filling material, or with more complex material models.

Although most real double wall constructions also incorporate some amount of mineral wool or other filling, partly for thermal and partly for acoustical insulation, it is still of interest for benchmarking purposes to model an empty double-wall. For all other cases when the cavity includes some amount of sound absorbing filling, the situation becomes different and the acoustic effect of the cavity will depend mostly on the material properties of the filling.

3.2 Creating models in AlphaCell

AlphaCell is a software for calculating sound transmission properties of a structure with Transfer Matrix Methodology (Allard & Atalla, 2009) (Matelys Research Lab, 2015). The program incorporates multiple acoustic modeling alternatives and handles calculation of thin plates, porous materials and double wall structures to name a few.

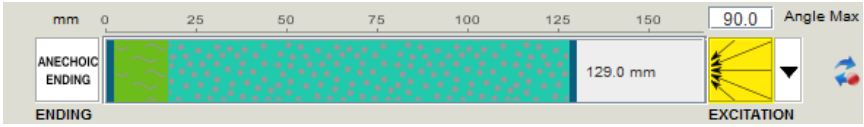

Figure 3.2: Double wall model in AlphaCell. From left to right: Anechoic ending, steel plate, air, filling material, steel plate, impinging wave field.

When creating a new model, the user needs to determine what type of different layers the modeled structure should have. AlphaCell contains a database with material properties to assign to each layer. New database objects can easily be created to contain the properties of customized materials. A schematic view of the model is visible in the top part of the program window, as shown in Figure 3.2, and displays the different layers that have been included.

The program incorporates different spatial windowing algorithms that can be applied to the model.

Figure 3.3 presents the results when modeling a double wall with TMM in AlphaCell. As is seen, infinite theory of single and double walls corresponds well with each other at low frequencies. When applying the spatial window technique on these walls, the calculated transmission loss is significantly increased at low frequencies. Material specifications for the modeled walls are presented in Table 3.2 below:

Table 3.2: Material properties of walls in Figure 3.3.

		Single wall	**Double wall**
Steel plate(s)	Thickness [m]	0.004	0.002
	Surface area [m^2]	2.0 x 2.0	2.0 x 2.0
	Poisson's ratio [-]	0.28	0.28
	Young's modulus [GPa]	200	200
	Density [kg/m^3]	7800	7800
	Loss factor [-]	0.01	0.01
Cavity	Hydraulic radius [m]	-	0.1
	Depth [m]	-	0.050

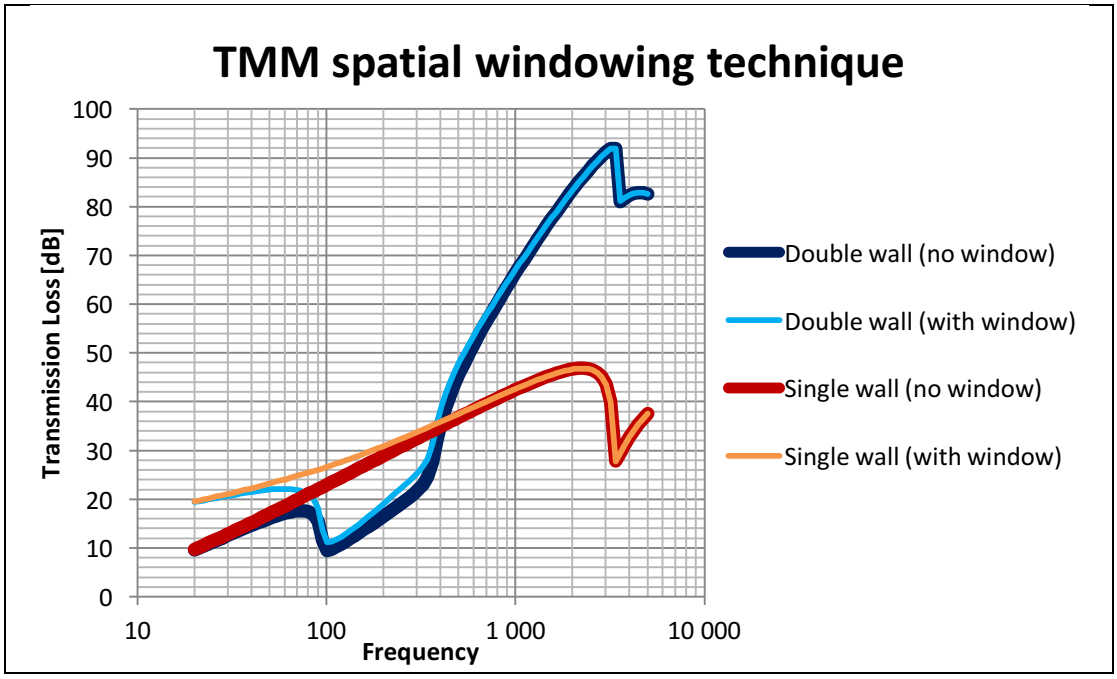

Figure 3.3: Modeling in AlphaCell. Transmission loss with and without spatial windowing. Both walls have the same mass.

3.3 Creating models in VA-One

VA-One is a vibro-acoustic software that enables modeling with both SEA and FE methodology. It is also possible for the program to handle Hybrid FE-SEA and BE calculations. Models are made in VA-One by creating structural objects that are connected through junctions. Each structural object in the model can be modified to have certain material properties that correctly represents the real structure. It is also possible to include air cavities, which is needed when modeling a double wall. To begin calculations, the model needs to include source objects. Receivers are included in the model to capture the response of SEA subsystems or at FE or BE nodes from the source input. The program calculates the response by solving the resulting system of equations representing the model.

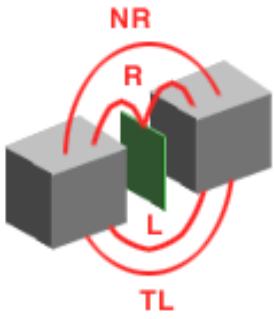

Figure 3.4: Illustration of the different paths sound can be transmitted in VA-One transmission suit model.

A SEA model is made out of several subsystems that are interconnected for the transmission of energy, see Section 2.4.1. However, the physical interaction between two plates in a double wall is not correctly represented when simply connecting a cavity directly with the plates on both sides. To account for the double wall effect of internal resonances, the VA-One software has a built-in Double Wall Junction (DWJ) that lets the user connect the plates to each other via the cavity.

Figure 3.5 illustrates the Double-Wall Junction in VA-One with the three paths T1, T2 and T3 that together form the non-resonant transmission paths. T1 connects the room cavities directly and often dominate the total flow of energy at low frequencies, near the double wall resonance. T3 couples one of the plates across the cavity to the air on the other side of the opposing plate, and typically dominate the total flow of energy close to the coincidence frequency. T2 connects the two plates directly with each other, representing the effect of e.g. structural elements connecting the two plates.

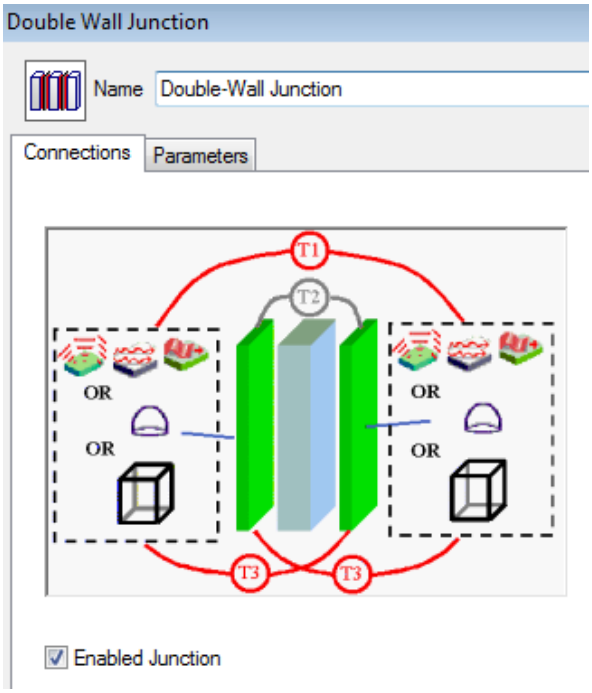

Figure 3.5: Screenshot of Double-Wall Junction menu in VA-One. T1 connects the cavities on both sides of the double wall. T3 couples one of the plates across the cavity to the air on the opposing side of the double wall. T2 is implemented manually.

The effects of the Double Wall Junction in a VA-One simulation are illustrated in Figure 3.6. The simulations were made with material properties as described in Table 3.3. The effects of including the double wall junction is substantial, with more than 20 dB reduction of the transmission loss at the double wall resonance.

Table 3.3 Material properties of walls in Figure 3.6.

		Single wall	Double wall
Steel plate(s)	Thickness [m]	0.003	0.0015
	Surface area [m^2]	4.0 x 8.0	4.0 x 8.0
	Poisson's ratio [-]	0.28	0.28
	Young's modulus [GPa]	200	200
	Density [kg/m^3]	7800	7800
	Loss factor [-]	0.01	0.01
Cavity	Average absorption [%]	-	1
	Depth [m]	-	0.020

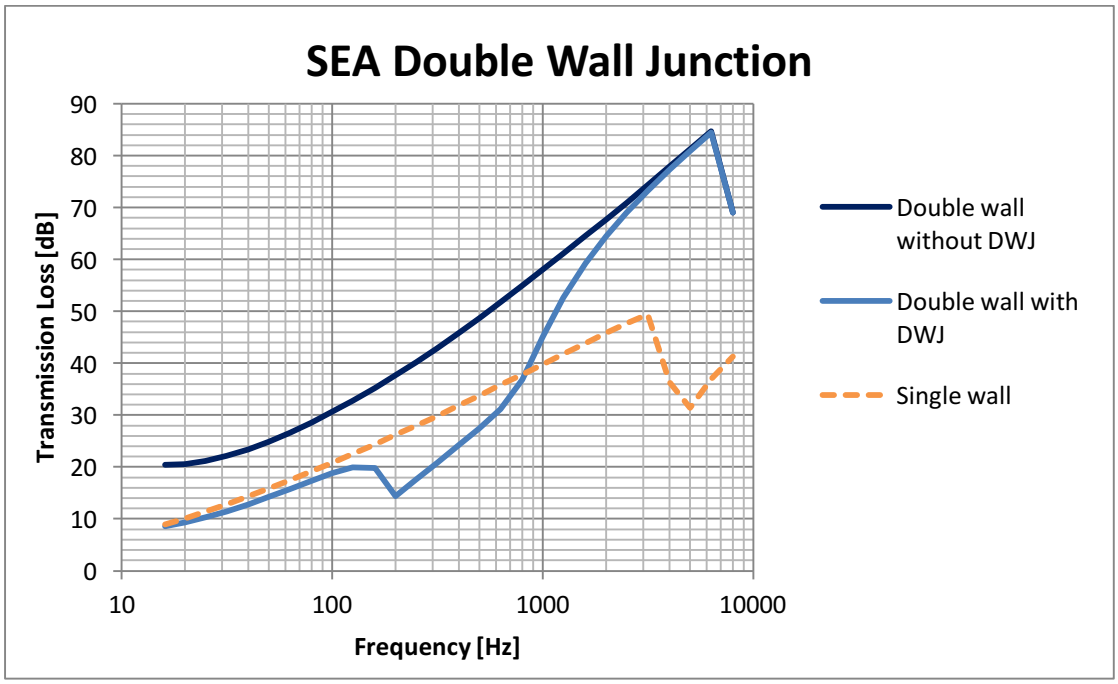

Figure 3.6: Modeling in VA-One. Double wall predictions are made with and without Double Wall Junction. The dashed line is a single plate with the same mass as the double wall. Material properties according to Table 3.3.

3.4 Refining the models: Effect of short circuiting

It was found in the early stages of the modeling procedure that both SEA and TMM predictions overestimated the transmission loss above 1 kHz. It is reasonable that some short-circuiting should occur between the plates in the test situation, and that the models are not incorporating this automatically. Short-circuiting happens because of mechanical edge effects at the plate edges, but also to some extent because the fluid near-field connects the two vibrating plates at frequencies around and below the coincidental frequency (Barbagallo, 2013).

To account for the mechanical short-circuiting that occurs at the plate edges, both VA-One and AlphaCell models were complemented with a spring element with stiffness k_y that connects the two plates. Different values on k_y were tried, but finally k_y= 8 kN/m was chosen as the model results best matched the measured results with this value. Figure 3.8 shows the effect when including the spring element. Insertion of spring elements modifies the T2 path illustrated in Figure 3.5.

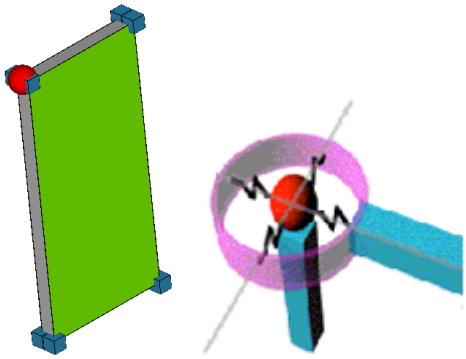

Figure 3.7: Illustrating the spring element inserted in the models.

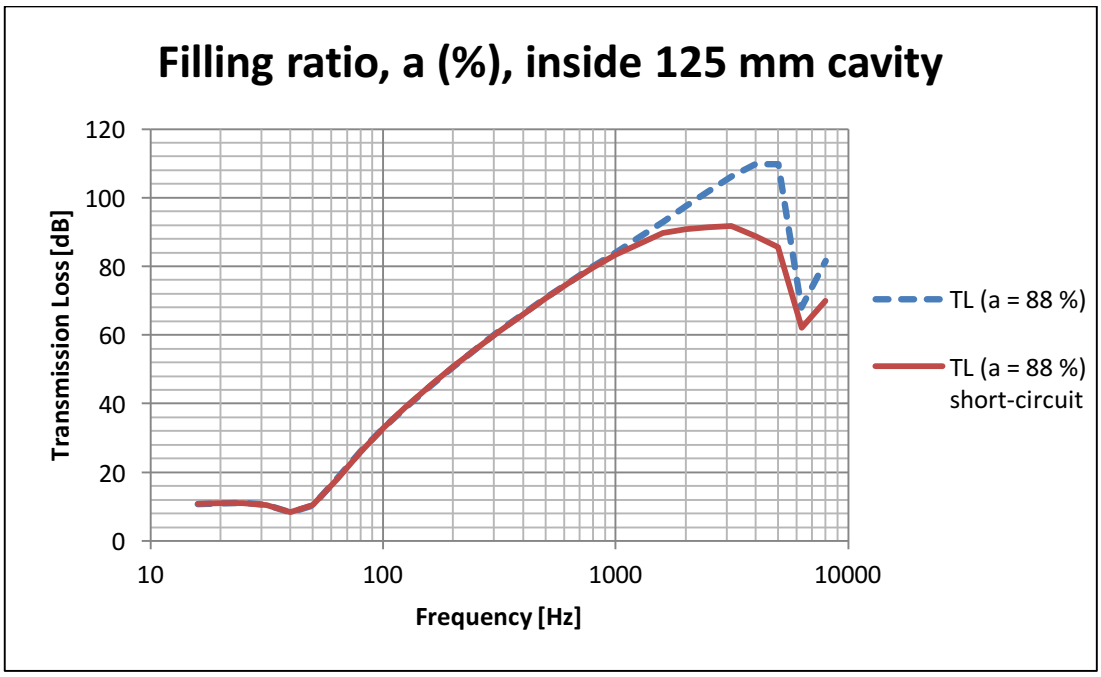

Figure 3.8: Including a spring element with stiffness ky= 8 kN/m in the SEA model to account for short-circuiting between the vibrating plates.

It is also possible to incorporate the mechanical short-circuiting effects in the AlphaCell model, by using a studded layer to represent the cavity. Such layers modifies the high frequency transmission but does not modify cavity resonances.

Hereafter, all double wall predictions include the short-circuiting mentioned.

3.5 Validating the prediction models

3.5.1 Effects when changing the filling ratio

In Figures 3.10 and 3.11 calculated and measured TLs are displayed for different filling ratios for double walls with a cavity depth of 125 mm. More results for a cavity depth of 50 mm is illustrated in Appendix A.

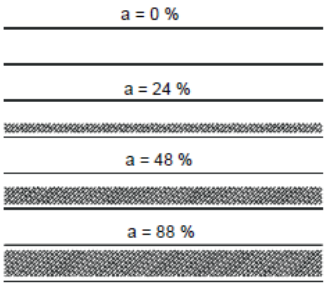

Figure 3.9: Illustrating the difference in filling ratio (Hongisto et. al., 2002).

The measurement data with filling material in the cavity reaches a plateau between 800 Hz and 2 kHz. Hongisto et. al. (2002) tries different hypotheses to explain the existence of the plateau but dismisses them all and the origin of the plateau remains unknown. Note that for other test setups, e.g with a 25 mm cavity depth, no plateau was observed. For these reasons, measurement data for walls with filling material inside is not included above 800 Hz in Figures 3.10 and 3.11.

It is clear that both the SEA and TMM models are working at their best when the wall has some amount of filling inside. The greatest increase in transmission loss happens when going from an empty cavity to a cavity with a small amount of filling material inside. Once there is some filling inside the cavity, it does not give that much greater effect to add more material.

For the case of an empty cavity, the SEA predictions agree well with measured data above 400 Hz. Low frequency results are uncertain. This is probably due to insufficient modal overlap, as discussed in Section 2.4.2. SEA theory requires that each modeled subsystem contains a certain amount of modes for the frequency band analyzed. The modal overlap M of the empty double wall is presented in Figure 3.12 with M = 1 at 250 Hz. This suggests that TL results below 250 Hz have some errors, but the errors gradually decrease with increasing frequency (Craik, 1996), which is probably why the results are corresponding well with the measurements above 0.4 kHz.

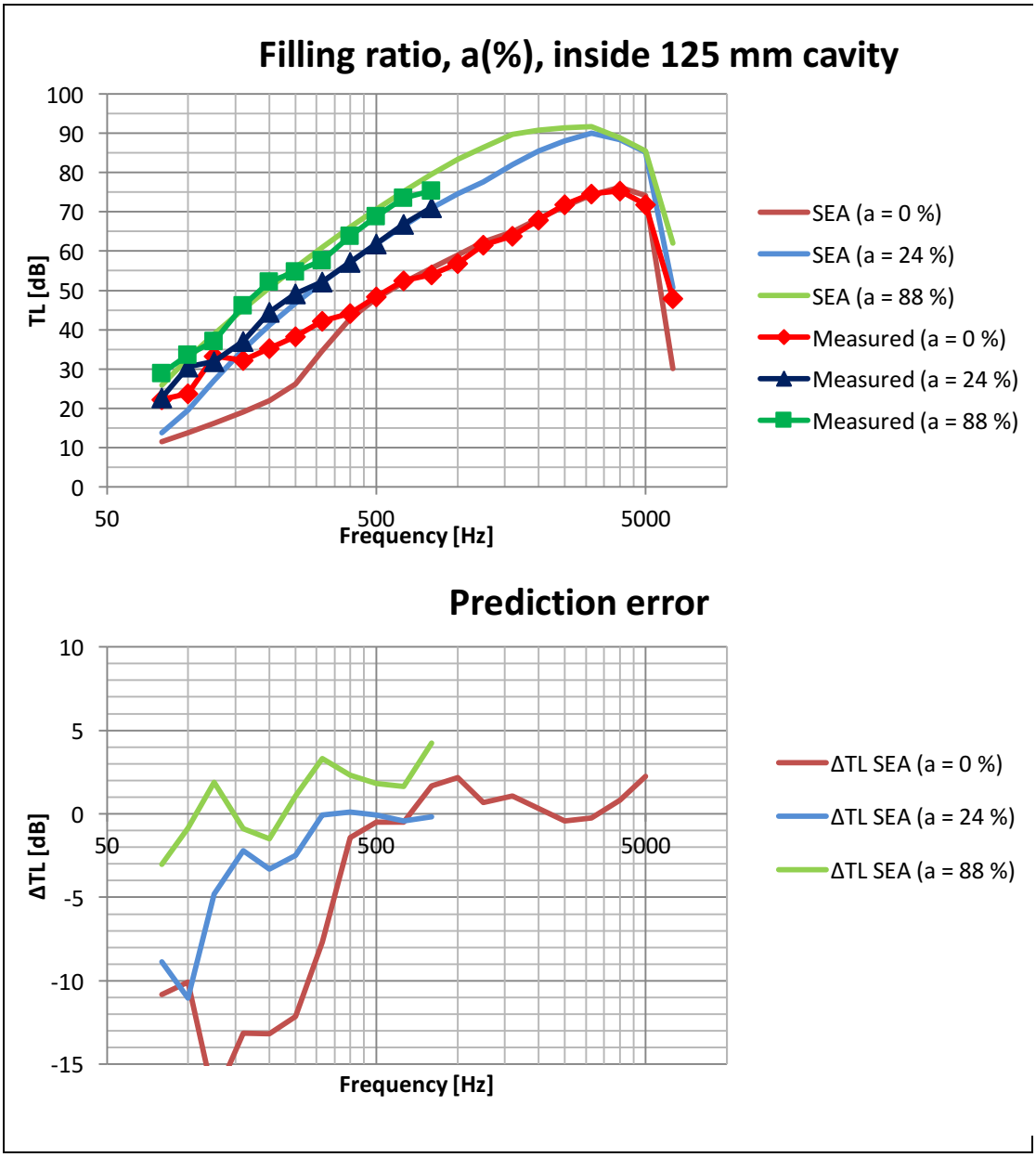

Figure 3.10: Comparing predicted SEA transmission loss with measurement data (Hongisto et. al., 2002) when changing the amount of filling material inside the cavity. (d = 125 mm ; σ= 8kPa·s/m2)

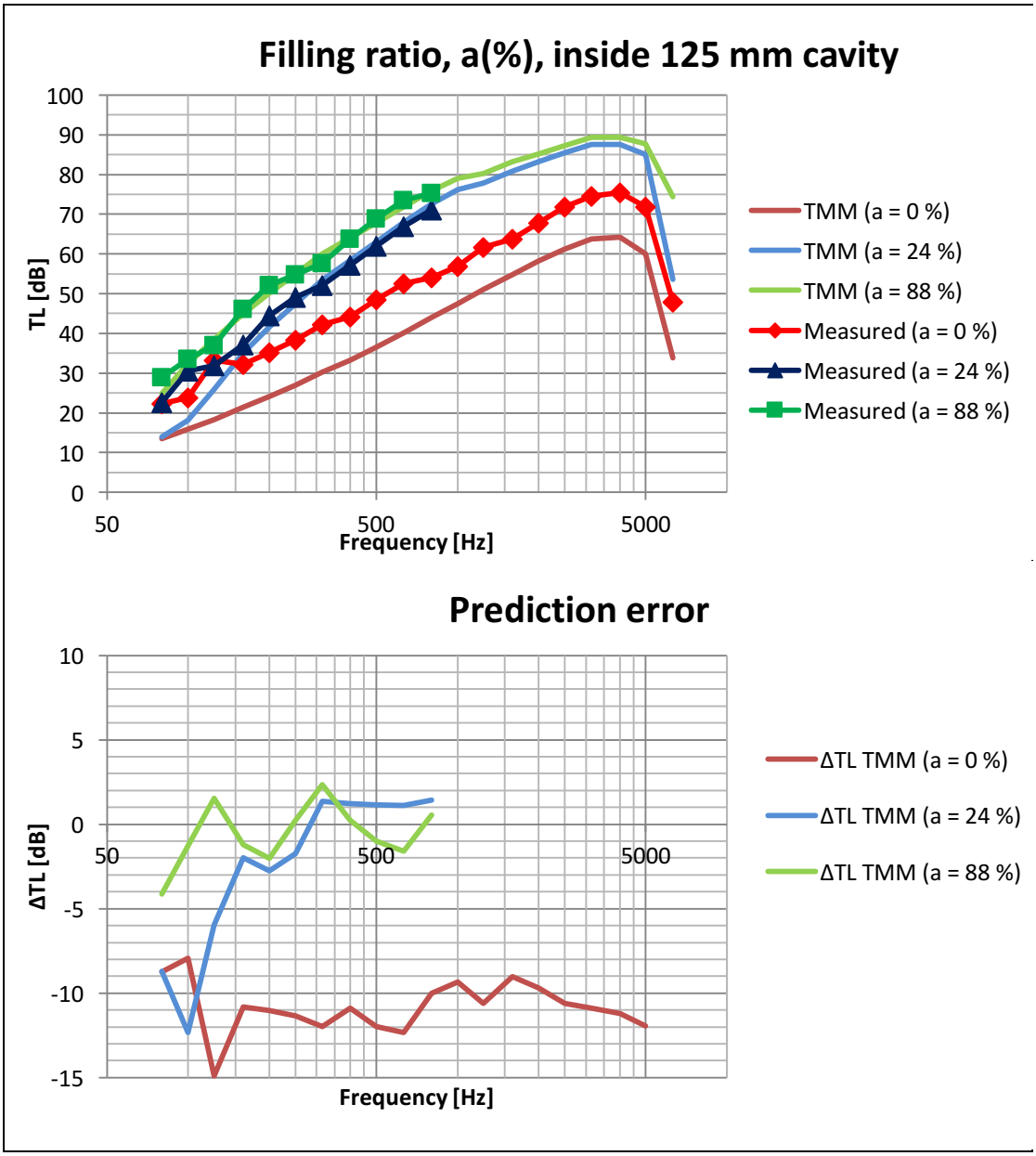

Figure 3.11: Comparing predicted TMM transmission loss with measurement data (Hongisto et. al., 2002) when changing the amount of filling material inside the cavity. (d = 125 mm ; σ= 8kPa·s/m2)

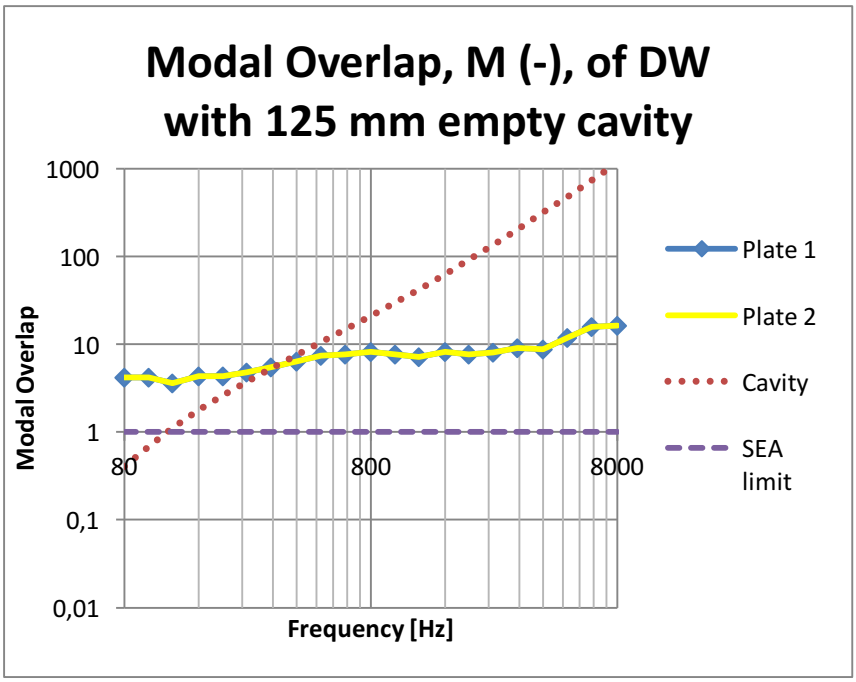

Figure 3.12: Modal overlap of double wall with empty cavity (d = 125 mm).

Considering the TMM predictions of a double wall without filling material, the results follow the same general trends as the measurements but underestimate the transmission loss by about 10 dB for all frequencies. This seems to happen due to limitations in how the model handles empty cavities. It is likely that the underlying problem is that cavity resonances cannot be correctly modeled in TMM due to the semi-infinite 2D geometry.

3.5.2 Effects when changing the air-flow resistivity of the filling material

The TL results when changing the air-flow resistivity of the filling material is presented in Figures 3.14 and 3.15. For these results the cavity is completely filled.

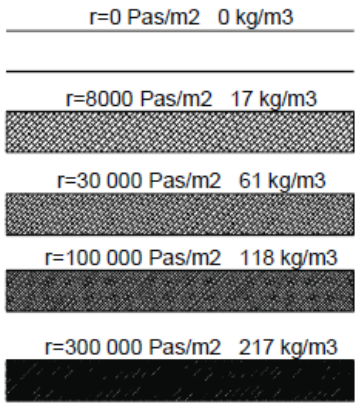

Figure 3.13: Illustrating the difference in air-flow resistivity (Hongisto et. al., 2002).

It appears that the transmission loss remains about the same for all configurations analyzed.

SEA results agree well with measurements when flow resistivity is set to 8 kPa·s/m^2. However, the results show overestimation at 30 kPa·s/m^2.

The TMM model predictions show good correlation with measurements. Again, the model overestimates the transmission loss when no filling material is used.

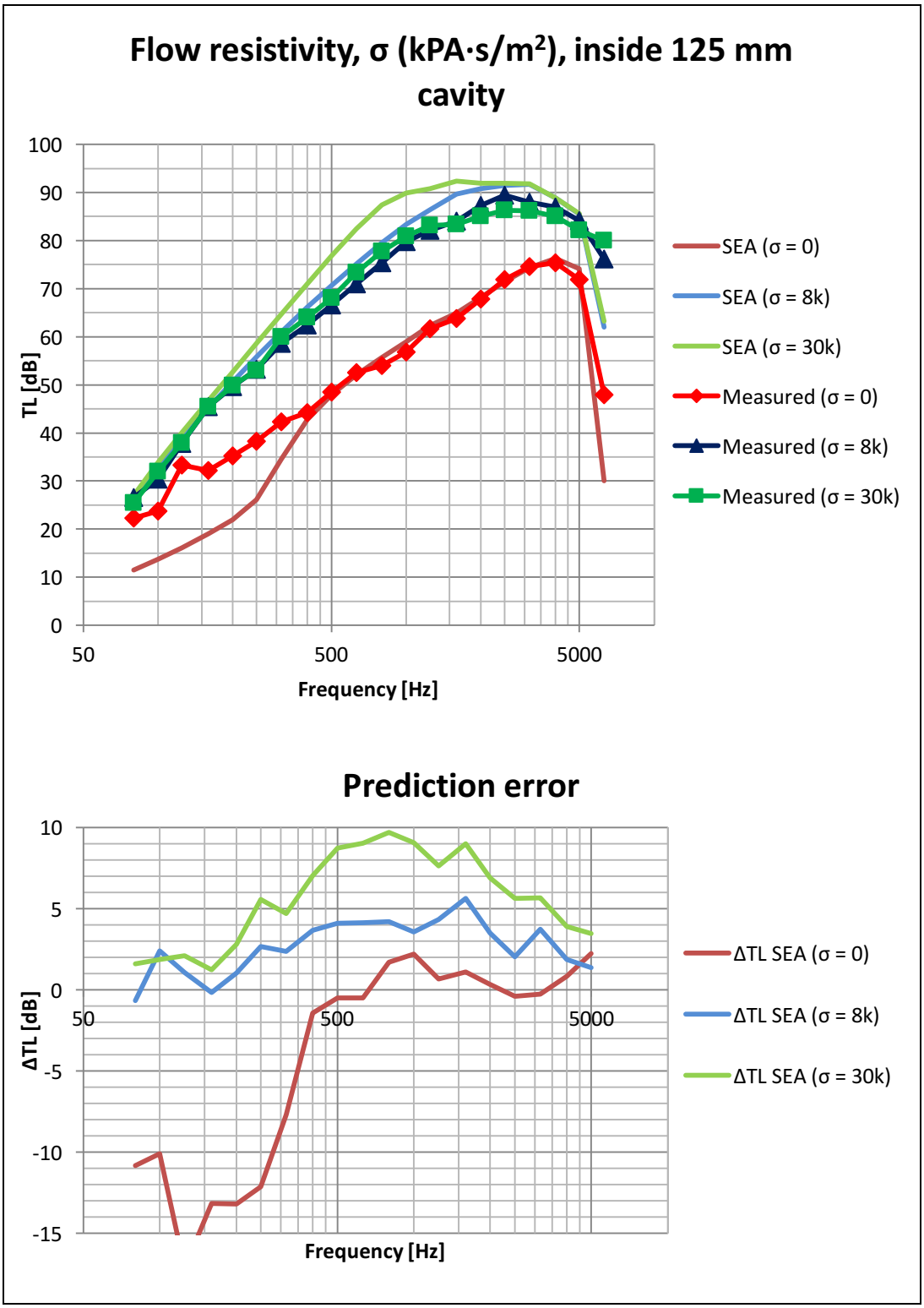

Figure 3.14: Comparing SEA transmission loss predictions to measured data (Hongisto et. al., 2002) when changing the air-flow resistivity of the filling material.

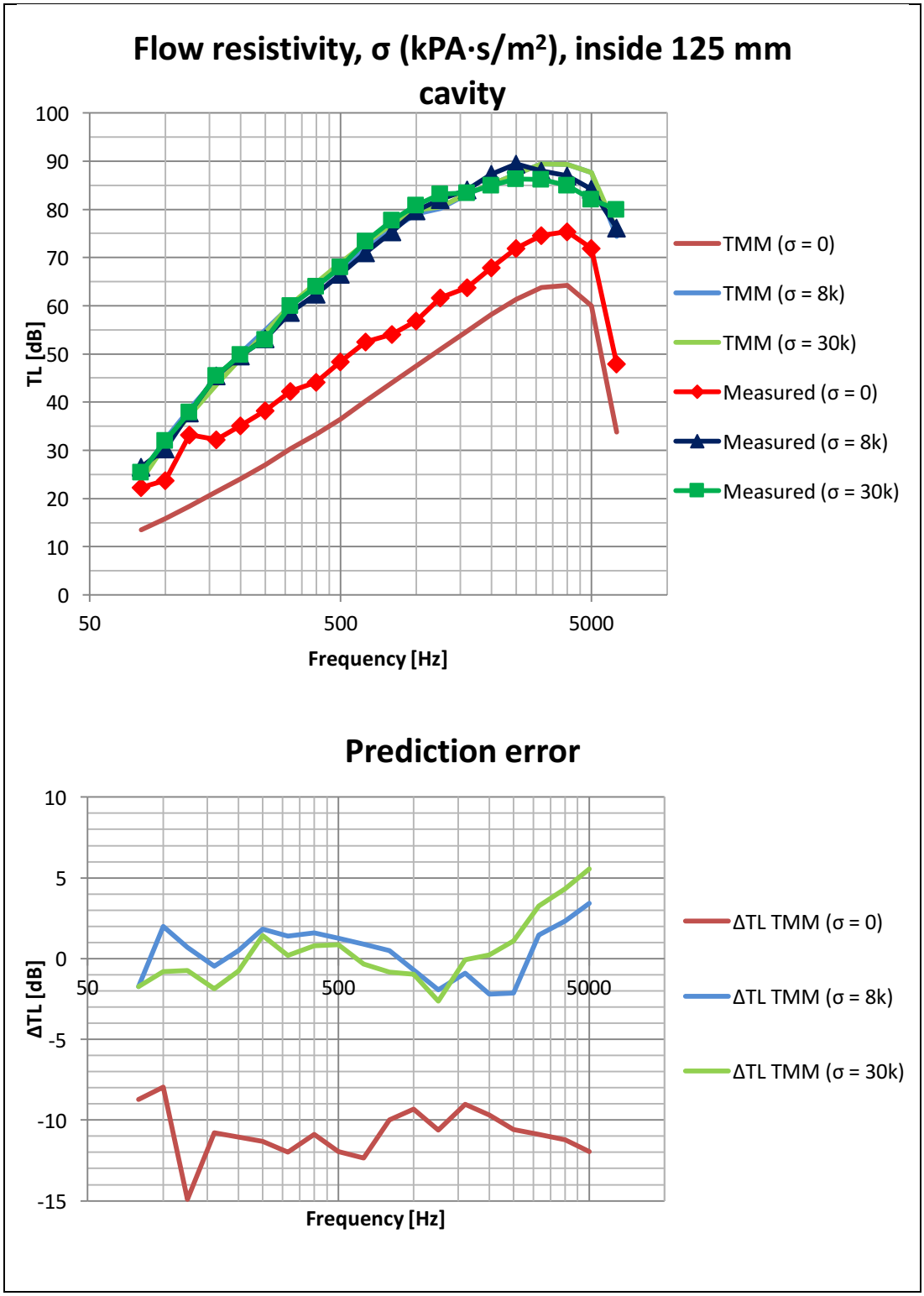

Figure 3.15: Comparing TMM transmission loss predictions to measured data (Hongisto et. al., 2002) when changing the air-flow resistivity of the filling material.

4 Train floor optimization

The final part of this thesis aims at solving a mass minimization problem of a structural floor typical for train cars. The purpose is to show the possibility to combine structural and acoustic constraints in the design process.

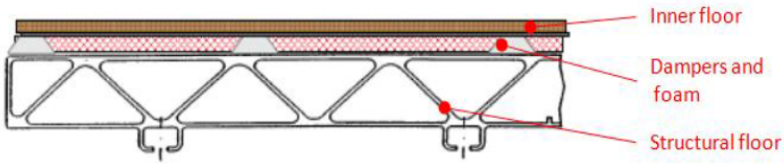

Figure 4.1: Cross-section of a train floor.

A train floor can be divided into three different layers, as illustrated in Figure 4.1. Much like a double wall, the train floor can be represented as two layers separated by a cavity that is partly filled with damping material. The structural floor is the foundation of the floor and will be the focus of the mass minimization problem in this thesis. This structural floor is designed using so-called extruded profiles which is a common solution for low weight and also reach a good pressure tightness of the rail car.

The aim of this minimization task is to show the possibility to combine structural and acoustic constraints when designing lightweight structures. The objective function is to minimize the mass per unit area of the structural floor, while also fulfilling constraints regarding deflection and sound transmission. The structural floor must be strong enough to hold the different loads that are applied, and provide enough sound insulation against incoming noise from under the train. However, combining both of these aspects can be difficult when striving to also minimize the mass.

Table 4.1 summarizes the optimization details. The same methodology applied in Chapter 2.5 can be used to describe the structural floor mass minimization problem at hand. Details regarding the specified parameters and constraints are presented in the following chapters.

Table 4.1: Presentation of the structural floor mass minimization task.

Objective function	Minimize the mass per unit area of the structural floor	m''
Parameters	Plate thicknesses	$t_{upper}, t_{inner}, t_{lower}$
	Geometrical cell size variables	L_x, L_z
Constraints	Deflection from static loads	δ
	A-weighted sound pressure level inside the train car	$L_{pA,inside}$

4.1 Approaching the optimization

There are multiple ways to approach the optimization problem at hand. The mass minimization task needed to have an overhead plan, for which different computer programs should control different subtasks in the optimization.

The optimization was broken down in the following subtasks:

- Create an acoustic numerical model of the train floor
- Calculate the deflection of the updated floor model using an analytical model
- Calculate the sound transmission of the updated floor model
- Update the model by changing some given parameters

The structural floor must be modeled in some computer program and a model geometry must be defined. To keep calculation time short, the computer model should be computationally effective, but still representative for the acoustic transmission properties of the entire floor.

Regarding the floor deflection, one alternative is to use a computer generated FE-model. This would however require long calculation times. For the purpose of this thesis, it was decided sufficient to use analytic equations of a freely supported beam to represent the train floor.

The task of calculating sound transmission was decided to be made with the VA-One software. Since the optimization should be working automatically, there was a need to combine all the different subtasks in one framework. It was decided that the main optimization routine should be written as a MATLAB script. This script should control other computer programs to work on separate subtasks. Since the scope of this thesis is limited in time, it would be helpful to use as few programs as possible. Every computer program requires a certain time for learning, and therefore it was preferred to use as few programs as possible. Furthermore, reducing the number of computer programs would also reduce the time needed to write a working MATLAB script that controls the different programs.

Having decided to use analytic beam equations to calculate the deflection, and using VA-One to calculate sound transmission, the entire optimization routine could be narrowed down to only incorporate MATLAB and VA-One. These two programs needed to be able to communicate with each other, and it was necessary to write separate code that translates all of the data given by MATLAB into information that could be read by VA-One. This turned out to be the largest task in this thesis.

The code that translates all commands given to VA-One from MATLAB was written in QuickScript, which is a programming language based on Visual Basic.

4.2 Constructing the floor optimization model

A model of a typical structural floor had previously been constructed in VA-One and was used for this optimization task. To improve calculation speed and simplicity in this optimization, the original model was reduced into a smaller cell as displayed in Figure 4.2. This means that the floor structure was taken to be periodic, and composed of a number of such cells repeated adjacent to each other. The structural cell would then be the focus for the remainder of this optimization task.

The method of calculating sound transmission with the periodic method has been proven successful in other similar applications. For further reading on the Periodic Cell calculation approach, see reference (Orrenius, 2009).

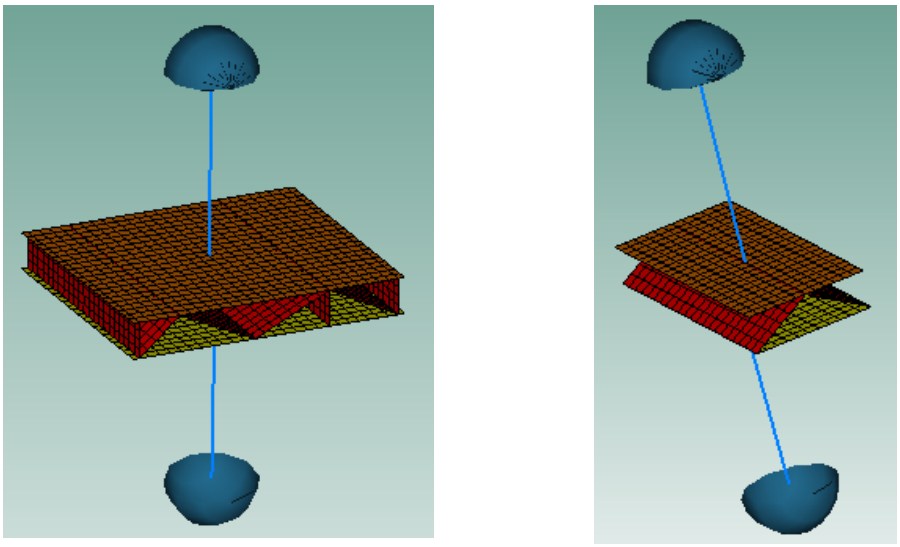

Figure 4.2: Original structure (left) and the simplified cell geometry (right)

Figure 4.3 shows the cell along with the five different parameters that were allowed to change over the course of the optimization. The parameters were defined as three different plate thicknesses (t_{upper}, t_{inner} and t_{lower}) and two geometrical cell size variables (L_x and L_z).

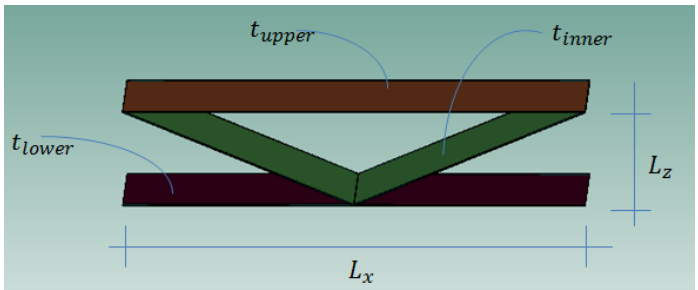

Figure 4.3: The structural cell used for the optimization illustrated with paramaters.

The cell model was created in VA-One with SEA plates in a design space that allows the parameters to be changed over a span of values within their corresponding bounds. The parameters and corresponding bounds are defined according to Table 4.2.

Table 4.2: Optimization parameters and their corresponding bounds.

Lower limit [mm]	Parameter	Upper limit [mm]
50.0	L_x	300.0
20.0	L_z	60.0
1.0	t_{inner}	5.0
1.0	t_{upper}	5.0
1.0	t_{lower}	5.0

This cell is the core of the optimization, where the objective function is to minimize the mass per unit area. The optimization routine allows the cell to be periodically replicated 15x15 times in the xy-plane to form a complete structural floor. This allows for transmission loss calculations, to find the corresponding A-weighted SPL inside the train. This was accomplished with the *Periodic module* in VA-One that automatically creates a periodic model from the structural cell. For this task, the *Periodic module* requires the structural cell to be meshed with a FE-grid.

The optimization routine works over a series of iterations to find the optimal solution that fulfills the defined constraints. Below is a presentation of what happens every iteration:

(1) MATLAB sets the new parameter values based on the outputs of the *fmincon* routine (see Section 2.5.3)
(2) MATLAB starts and operates VA-One in the background
(3) VA-One uses the parameter values to update the cell geometry
(4) The updated VA-One model is meshed and the mass is calculated
(5) VA-One replicates the cell geometry over the xy-plane into a larger area and calculates the TL of the resulting structural floor
(6) MATLAB closes VA-One
(7) MATLAB uses the calculated TL in post-processing to find the A-weighted SPL inside the train car
(8) MATLAB calculates the deflection of the structural floor
(9) Compare (7) and (8) with the specified constraints

Each iteration involves a number of different sub-processes (3)-(8), in which computation is made with new parameter values. In step (1) *fmincon* is used to find the gradient of the objective function to determine the parameter vector for the next iteration. If the constraints are not met in step (9), the optimization script changes the parameters and updates the geometry to make a new calculation to iteratively find a parameter vector for which both constraints are met. For details on how the parameters are changed, see Arora (2004).

When both constraints have been met, the optimizer continues to change the parameters to minimize the mass still respecting the constraints. As the optimizer runs this iterative process, the parameter values shall eventually converge into a final design solution for the optimized floor.

4.3 Completing the optimization routine

This optimization uses the original structure presented in Figure 4.2 with the material data as presented in Table 4.3 as starting point. The model was set up, to calculate the deflection and A-weighted sound pressure level inside the train car.

Table 4.3: Material properties of original structural floor

Aluminium plates	Thickness [mm]	2.8
	Young's modulus [GPa]	200
	Density [kg/m^3]	7800
	Damping loss factor [%]	2

The maximum deflection due to a distributed static load was calculated with analytic equations for a freely supported beam,

$$\delta = \frac{5qL^4}{384EI} \qquad (25)$$

where δ [m], is the deflection at the mid-point, q is the distributed load [N/m], L is the length of beam [m], E is the Young's modulus and I [m^4], is the moment of inertia.

The moment of inertia of the structural floor was calculated according to formulas presented by Kohrs (2002), see Equations (26) - (29). Here, $I'_{y,tot}$ is the total moment of inertia, calculated as the sum of the moment of inertia of inner $I'_{y,inner}$ and outer plates $I'_{y,outer}$. Examples of plate thicknesses t_a and t_i are shown in Figure 4.5 along with structural floor height h.

This method makes it possible to approximate the structural floor of the train as a beam, to calculate the deflection using standard beam theory. The main assumption is that of the free edges. Generally speaking, the flexural stiffness of the walls will add rotational stiffness at the floor/beam edges, meaning that the assumption of free edges leads to a conservative estimate of the floor deflection. For the optimization problem, the structural floor was assumed to hold a distributed load of 500 kg/m^2, representative to the passenger load of a fully loaded metro car.

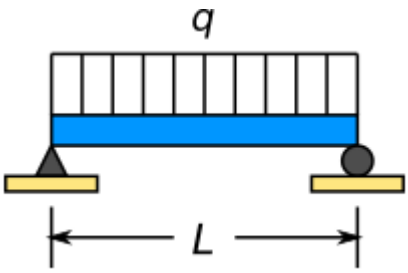

Figure 4.4: Freely supported beam with a distributed load. Used as an approximation to calculate the static deflection of the structural floor.

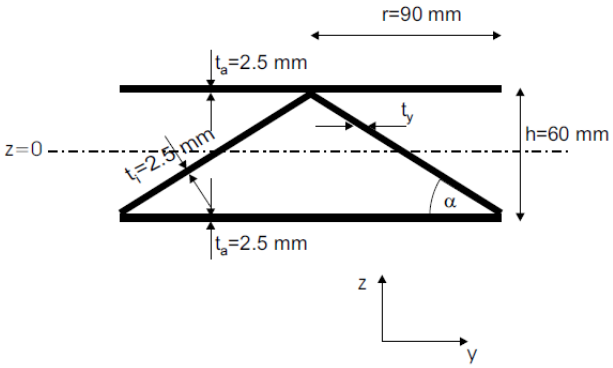

Figure 4.5: Example of cell geometry when calculating Youngs Modulus for a floor made of extruded plates (Kohrs, 2002)

$$I'_{y,tot} = I'_{y,outer} + I'_{y,inner} \tag{26}$$

$$I'_{y,outer} = 2\left(\frac{t_a^3}{12} + \left(\frac{h - t_a}{2}\right)^2 \cdot t_a\right) \tag{27}$$

$$t_y = \frac{t_i}{\sin\alpha} = \frac{t_i}{\sin\left(\tan^{-1}\left(\frac{h - t_a}{r}\right)\right)} \tag{28}$$

$$I'_{y,inner} = \frac{1}{b}\int_A z^2 dA = \frac{1}{b}\int_{-(\frac{h}{2}-t_a)}^{\frac{h}{2}-t_a} z^2\left(t_y \cdot dz\right) \tag{29}$$

Equation (27) is based on that the profile is symmetric, i.e. t_a=t_b. However, the optimization routine is allowed to change all plate thicknesses independently, meaning that the upper and lower plates can have different thicknesses. Since calculations were made with the equations above, it leads to incorrect values for the moment of inertia. This was an unfortunate error that was discovered late in the project, with little time to make any changes. However, this does not affect the main result of this thesis: that both acoustic and structural constraints can effectively be used when optimizing a floor construction for minimum weight.

The A-weighted SPL inside the train car is defined with the same premise as in Equation (10), and is calculated as,

$$L_{pA,inside} = L_{pA,outside} - TL + 10\log_{10}\frac{S}{A} \qquad (30)$$

where $L_{pA,outside}$ is the sound level in the bogie cavity, here taken as a typical spectrum measured in the motor bogie for a train at 90 km/h with a strong peak at 1250 Hz as shown in Figure 4.6. Based on the properties of this spectrum, the frequency range was taken as 100-3150 Hz. The train car interior is simplified into a room with dimensions 3x3x2.5 m^3 where all surface areas are assumed to have an absorption coefficient of 0.28, defining the absorption area A. The separating surface area S is in this case set to a 3x3 m^2 square.

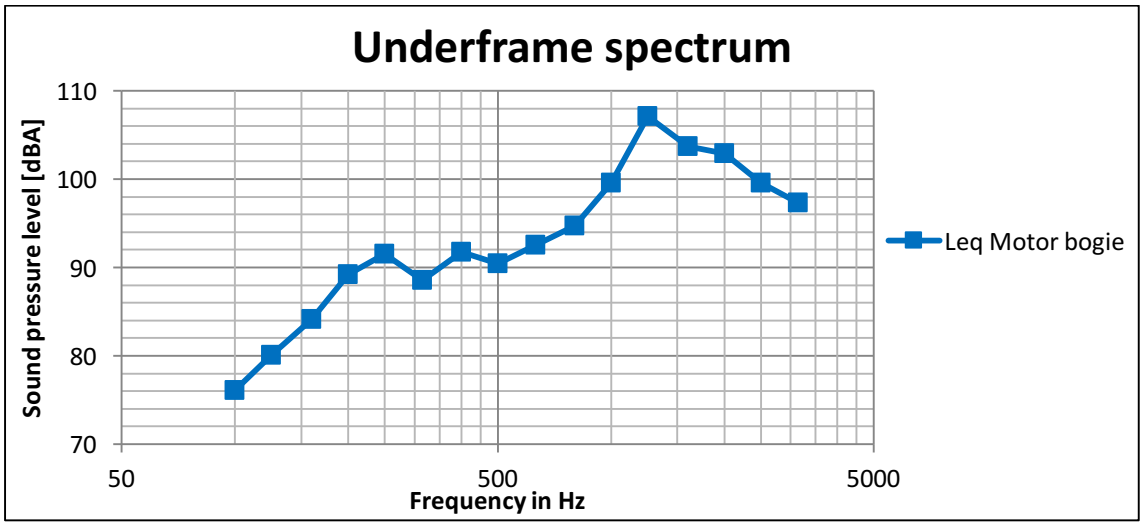

Figure 4.6: Underframe spectrum representing the noise source underneath the train floor.

VA-One calculates the mass of all plates in the model. The total mass (kg) of all plates is divided by the cell area to generate the objective mass per unit area.

Table 4.4 presents the calculated deflection according to Equation (25) and the associated A-weighted SPL in the receiving room from Equation (30) for the original floor which are taken as the optimization constraints. This means that any new design must be at least as good as the original design.

Table 4.4: Calculated deflection and A-weighted SPL inside the train car of the original structure.

Deflection from static loads	δ = 17.6 mm
A-weighted SPL inside the train car	$L_{pA,inside}$ = 80.2 dBA

Note that $L_{pA,inside}$ accounts for sound transmission through the structural floor. The noise level will be reduced when also the inner floor is included, see Figure 4.1.

4.4 Optimization results

The optimization begins at a given starting point. Figure 4.7 presents the results of the iterations when setting the starting point at either the upper (B) or the lower (A) parameter bounds according to Table 4.2.

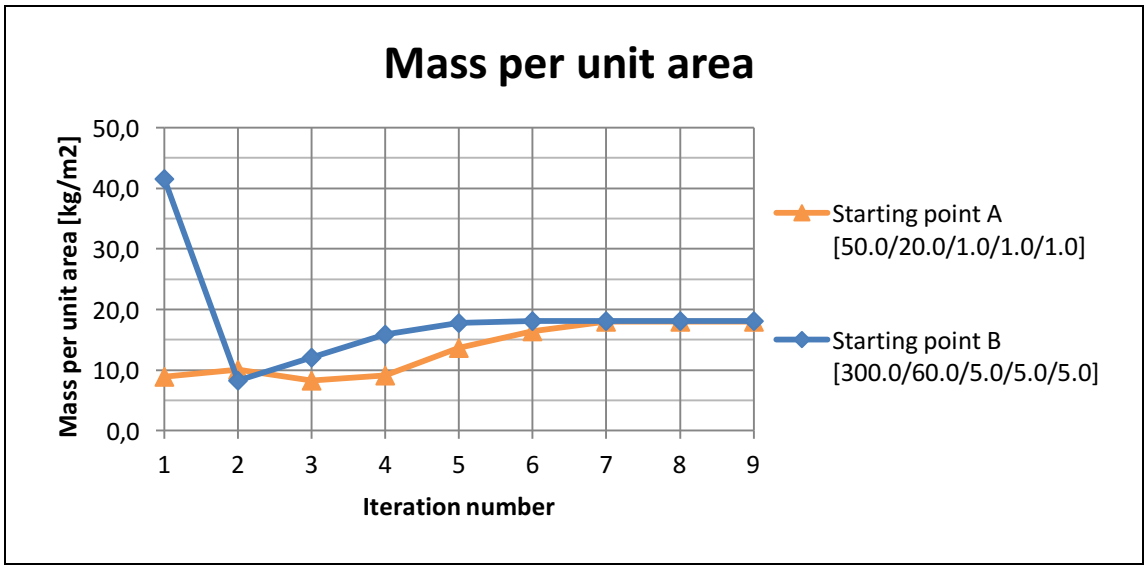

Figure 4.7: Floor mass when starting at A or B. Parameter values: $L_x/L_z/t_{inner}/t_{upper}/t_{lower}$.

The final point of convergence is the same for both simulations, 18.0 kg/m^2, strengthening the conclusion that a global minimum is found.

Figure 4.8 presents the parameter values at each iteration and the corresponding mass per unit area. Parameters of point A is taken as starting point.

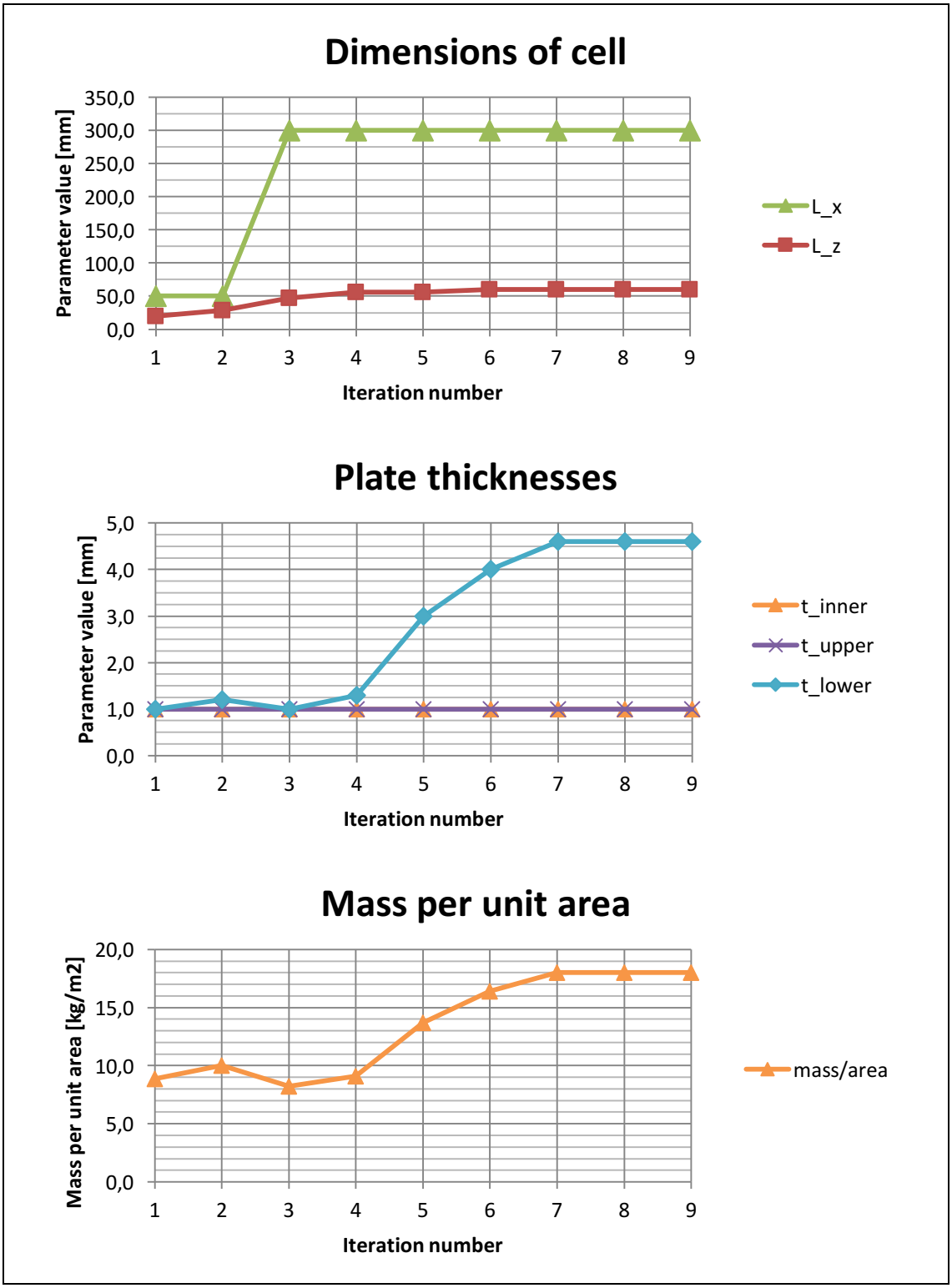

Figure 4.8: Illustrating the trend of parameter values and the objective function as the optimization runs over several iterations.

4.5 Analysis

The results in Figure 4.8 show that the final design is strongly asymmetrical, with one of the outer plates much thicker than the other one. Table 4.5 compares the optimized structure with the original one.

Table 4.5: Optimization results

	L_x [mm]	L_z [mm]	t_{inner} [mm]	t_{upper} [mm]	t_{lower} [mm]	m'' [kg/m^2]
Original geometry	190.0	57.5	2.8	2.8	2.8	23.8
Final geometry	300.0	60.0	1.0	1.0	4.6	18.0

To check this design solution, further investigations were made to learn how the transmission loss varies with the mass ratio of the two outer plates. These complementary results are presented in Figure 4.9 and show the transmission loss of four different panels: i) the original structure, ii) the final structure, iii) the final structure flipped "upside-down", iv) a symmetric structure with the same mass per unit area as the final design.

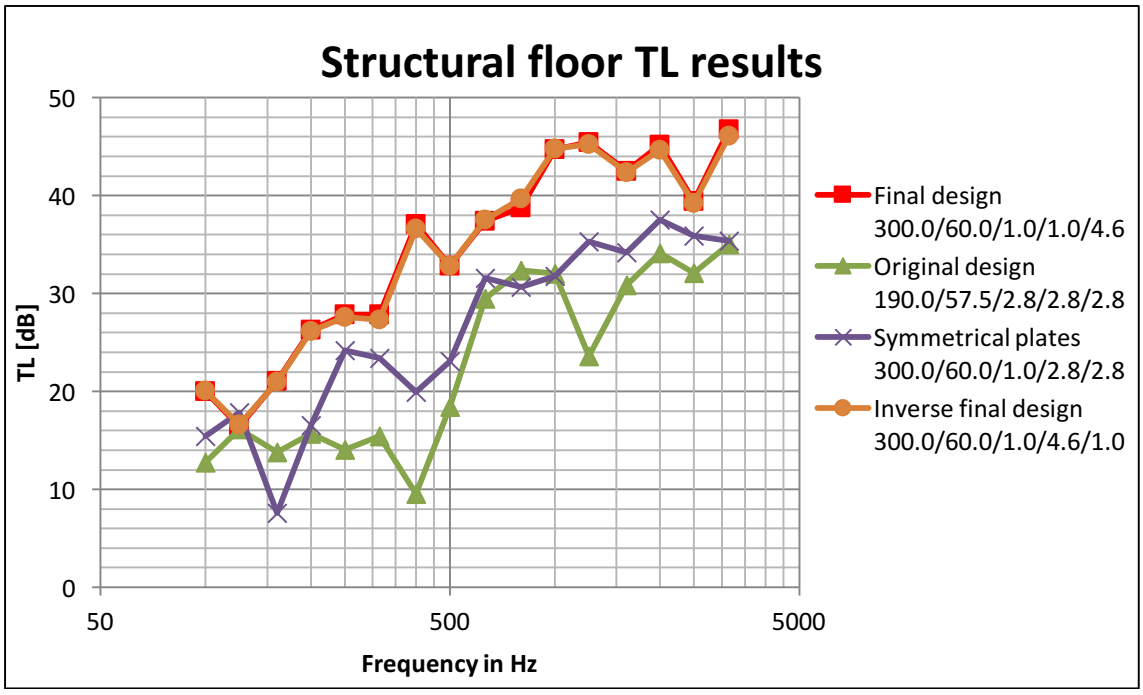

Figure 4.9: Transmission loss results for different design solutions. The parameters of each design are stated as: $L_x/L_z/t_{inner}/t_{upper}/t_{lower}$.

These results confirm that the transmission loss is largest with an asymmetrical design. Approximately the same TL results were obtained when inverting the outer plate thicknesses of the original design, i.e. turning the final design upside down. Also shown is that the transmission loss is significantly decreased when changing the mass ratio of the final design so that the outer plates are of equal thickness. It is also notable that for the final design the TL has been significantly improved at 1250 Hz compared to the original design, which is the frequency band with the highest input noise levels. It is possible that the optimization routine favors design solutions that succeed in suppressing the peak level of the incoming sound.

Figure 4.10 shows calculated radiation efficiencies of the upper and lower side of the structure for the original design and the final one. The radiation efficiency of the upper plate is significantly decreased for the final design. As it is very thin, the hypothesis is that it therefore has a weaker coupling to the fluid resulting in a lower radiation efficiency, thus improving the TL of the entire floor.

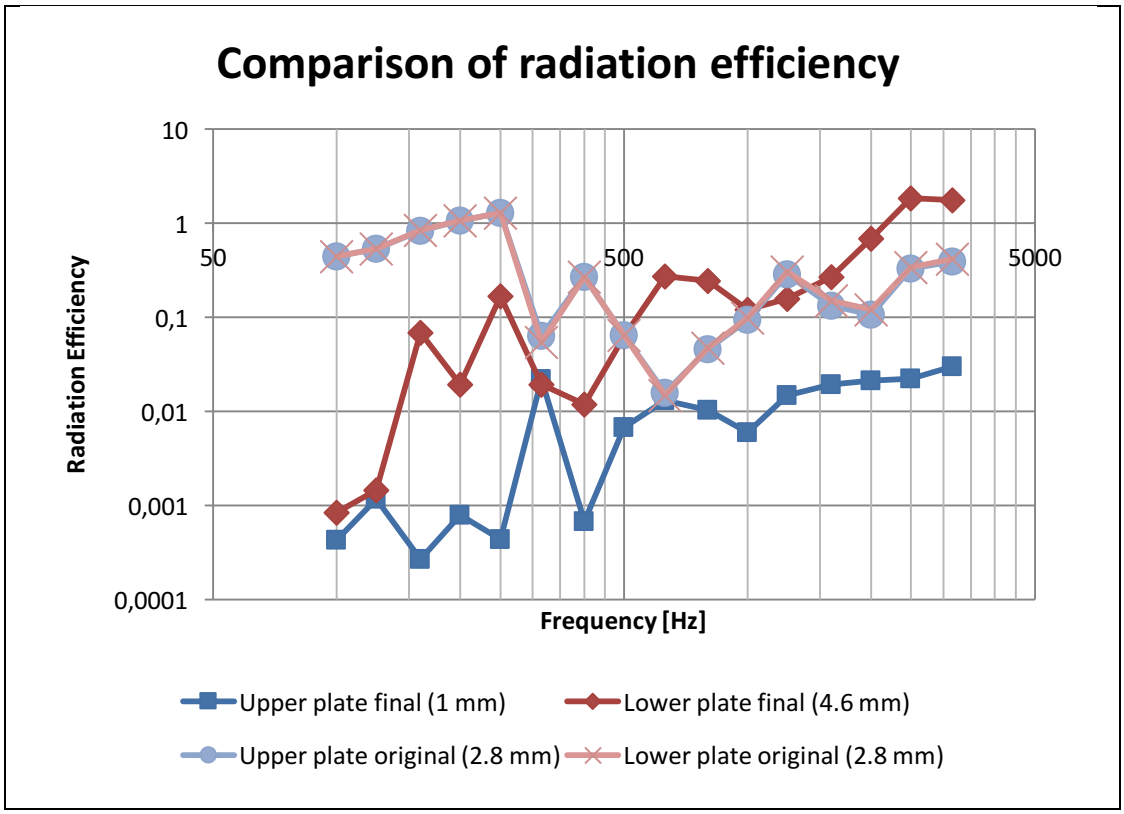

Figure 4.10: Radiation efficiency of the upper and lower plates of the original and the final design, calculated using the VA-One model.

5 Discussion

This thesis is divided in two parts; double wall modeling and structural optimization. The common denominator for the two parts is the extensive work with VA-One. It is very important to understand how the program operates, and it was necessary to begin the thesis with a stand-alone task to model double walls before beginning the actual optimization task.

5.1 Double wall modeling

Computer programs VA-One (SEA) and AlphaCell (TMM) were used to create two different double wall models.

To account for the mechanical short-circuiting that occurs at the plate edges, both SEA and TMM models were complemented with a spring element that connects the two plates. The SEA model also incorporates a Double Wall Junction that is a built in tool in VA-One, specifically used to represent the double wall effect of internal resonances. To improve the TMM model, a spatial windowing algorithm was applied to account for the finite size of the double wall.

Both SEA and TMM models agree well with measurement data. It was noted that the TMM model was limited when modeling a cavity without filling material, because in-plane resonances in the cavity cannot be accurately modeled due to the semi-infinite geometry the TMM relies on. It is possible that the damping properties of the empty cavity could be better estimated by including a very small amount of filling material in the TMM model, and thus make it a better estimation of the real empty cavity.

For future work on double wall modeling, it is recommended to evaluate and validate the effects when changing other parameters such as plate thicknesses.

5.2 Structural optimization

Working with optimization is a difficult task that requires a well thought-out plan that takes in consideration a large amount of details. This thesis aims at showing the possibility to combine constraints from different disciplines in the design process by including them in an optimization routine. To reduce the complexity, with regards to the time frame of the thesis, the routine needed to rely on a few simplifications. For future work, it is recommended to improve the routine by including a more detailed description of the static load cases when calculating the deflection. This could be done with a FE model of the structural floor. It is also recommended to include constraints on local deformations of the plates. Another possible improvement of the routine could be to use stress as the limiting structural constraint, or combining stress with static deflection and local deformations all together.

As described in Section 4.3, the optimization routine was created to allow all plate thicknesses to be changed independently. It was noted late into the project that, due to an unfortunate error, the Young's modulus was calculated with the same thickness on both upper and lower plates. However, this does not affect the main result of this thesis: that both acoustic and structural constraints can be effectively used when optimizing a floor construction for minimum weight.

Furthermore, it is also recommended to evaluate what would happen if the spectrum of the incoming noise would have been different. The spectrum used in this optimization had a peak at 1250 Hz, and as is stated in Section 4.4 the results suggests that the final design depends on where this peak is located.

If a similar optimization routine would be applied to find a design solution that could be taken directly into production, it is of absolute importance to have well defined constraints. This thesis worked with optimization in regards to a reference floor, where the constraints were defined such that the final design should not exceed the deflection of the original floor nor should it impair the sound insulating properties of the original floor. Thus, the constraints were defined in relation to the reference floor. Regarding a scenario where the optimization is used for commercial production, the constraints should preferably be set in absolute terms rather than in relative terms. This ultimately requires knowledge in what actually is a possible allowed deflection, under a specified load, if deflection should be used as a constraint. Working with such an optimization would also require either experimental or numerical validation to be certain that the optimization results can be trusted for production.

Similarly, the design variables should be defined such that they have upper and lower bounds that are directly applicable for production purposes. For instance, if using plate thicknesses as design variables, too thin plates could be problematic when regarding welding or if they would be damaged.

6 Conclusions

In the first part of the thesis a double wall was modeled with two different acoustic software in order to calculate the transmission loss and benchmark with measurement data. The aim was to develop validated transmission models for analysis of air-borne sound through train floors, which can be simplified into a double wall with absorptive filling material. The two models used SEA and TMM theory respectively to calculate transmission loss, and the models were subject to a parameter study to analyze effects when changing the amount of absorptive material inside the double wall and also when changing the air-flow resistivity of the absorptive filling material.

Having benchmarked both SEA and TMM models, it was shown that the calculated transmission loss results agree well with measurement data. Both models were complemented with a spring element that connects the two plates, to account for the mechanical short-circuiting that occurs at the plate edges. It was noted that the TMM model was limited when modeling a cavity without filling material, because in-plane resonances in the cavity cannot be accurately modeled because of the semi-infinite geometry the TMM relies on.

For the second part of the thesis, an optimization algorithm including acoustic and structural constraints was developed in MATLAB to minimize the mass of a train floor. The algorithm was set to calculate the static deflection of the train floor with analytic beam equations. A FE model of the train floor was created from a periodic cell of the structure and the acoustic transmission loss could be calculated by applying periodic boundary conditions. The optimization algorithm was written in regards to a reference floor, where constraints were defined such that the optimized floor should not exceed the deflection of the original floor nor should it impair the sound insulating properties of the original floor. The aim of the optimization task was to solve the mass minimization problem, however was not aiming at finding an optimal design solution ready for commercial use.

The results showed it was possible to combine the specified constraints and the optimization algorithm could solve the mass minimization problem. The optimization exercise gave some interesting results. Using an original floor structure with mass per unit area 23.8 kg/m^2 as reference, the optimization results in a final design with 18.0 kg/m^2. The optimized structure is highly asymmetric, and convergence is verified from two different starting points. For future work it is recommended to include a more detailed description of the static load cases when calculating the deflection. It is also suggested to evaluate if structural constraints could be defined to include a combination of stress, static deflection and local deformations.

7 Bibliography

Allard, J.F., Atalla, N (2009) *Propagation of Sound in Porous Media*. 2nd edition. Hoboken, N.J.: Wiley.

Arora, J.S. (2011) *Introduction to optimum design*. 3rd edition. USA: Elsevier Academic press.

Barbagallo, M. (2013) *Statistical energy analysis and variational principles for the prediction of sound transmission in multilayered structures*. Stockholm: KTH Royal Institute of Technology

Bartolozzi, G., Orrenius, U., Pratellesi, A., Pierini, M. (2012a) An Equivalent Orthotropic Plate Model for Sinusoidal Core Sandwich Panels in Optimization Processes, In *Noise and Vibration: Emerging Methods, NOVEM2012, 1-4 April 2012, Sorrento*

Bartolozzi, G., Pierini, M., Orrenius, U. (2012b) Handling of acoustic constraints in multidisciplinary optimization processes. In *International Conference on Noise and Vibration Engineering, ISMA2012, 17-19 September 2012, Leuven*

Craik, R. (1996) *Sound Transmission through Buildings using Statistical Energy Analysis*. Aldershot: Gower, cop.

ESI Group (2015), *VA-One: User's manual*

Fahy, F. (1985) *Sound and Structural Vibration – Radiation, Transmission and Response*. London: Academic Press.

Grosveld, F.W. (1985) Field-Incidence Noise Transmission Loss of General Aviation Aircraft Double Wall Configurations, *Journal of Aircraft*, vol. 22, no. 2, pp. 117-123

Hongisto, V., Lindgren, M. and Helenius, R. (2002) Sound Insulation of Double Walls – An Experimental Parametric Study, *Acta Acustica united with Acustica*, vol 88, no. 6, pp. 904-923

Kohrs, T. (2002) *Structural acoustic investigation of orthotropic plates*. Berlin: TU Berlin Institut für Technische Akustik

Lyon, R.H., DeJong, R.G. (1995) *Theory and application of statistical energy analysis*. 3rd edition. Newton: Butterworth-Heinemann.

Matelys Research Lab (2015), *AlphaCell: User's manual*

Orrenius, U., Cotoni, V., Wareing, A. (2009) Analysis of sound transmission through periodic structures typical for railway carbodies and aircraft fuselages. In *Noise and Vibration: Emerging Methods, NOVEM2009, 5-8 April 2009, Oxford*

Orrenius, U., Wareing, A., Kumar, S. (2010) Prediction and control of sound transmission through honeycomb sandwich panels for aircraft fuselage and train floors. In *The 10th International Congress on Sound and Vibration, ICSV10, 7-10 July 2010, Stockholm*

Tageman, K. (2013) *Modelling of sound transmission through multilayered elements using the transfer matrix method*. Göteborg: Chalmers University of Technology. Master's thesis.

Vigran, T.E. (2009) Predicting the sound reduction index of finite size specimen by a simplified spatial windowing technique. *Journal of Sound and Vibration*, vol. 325, no. 3, pp. 507-512

Villot, M., Guigou, C. and Gagliardini, L. (2001) Predicting the acoustical radiation of finite size multi-layered structures by applying spatial windowing on infinite structures. *Journal of Sound and Vibration*, vol. 245, no. 3, pp. 433-455.

Wennhage, P. (2002) Weight Optimization of Sandwich Panel with Acoustic Constraints, Experimental Verification, *Journal of Sandwich Structures and Materials,* vol. 4, no. 4, pp. 353-365

Appendix A

A.1 Parameter study on double wall, d = 25 mm

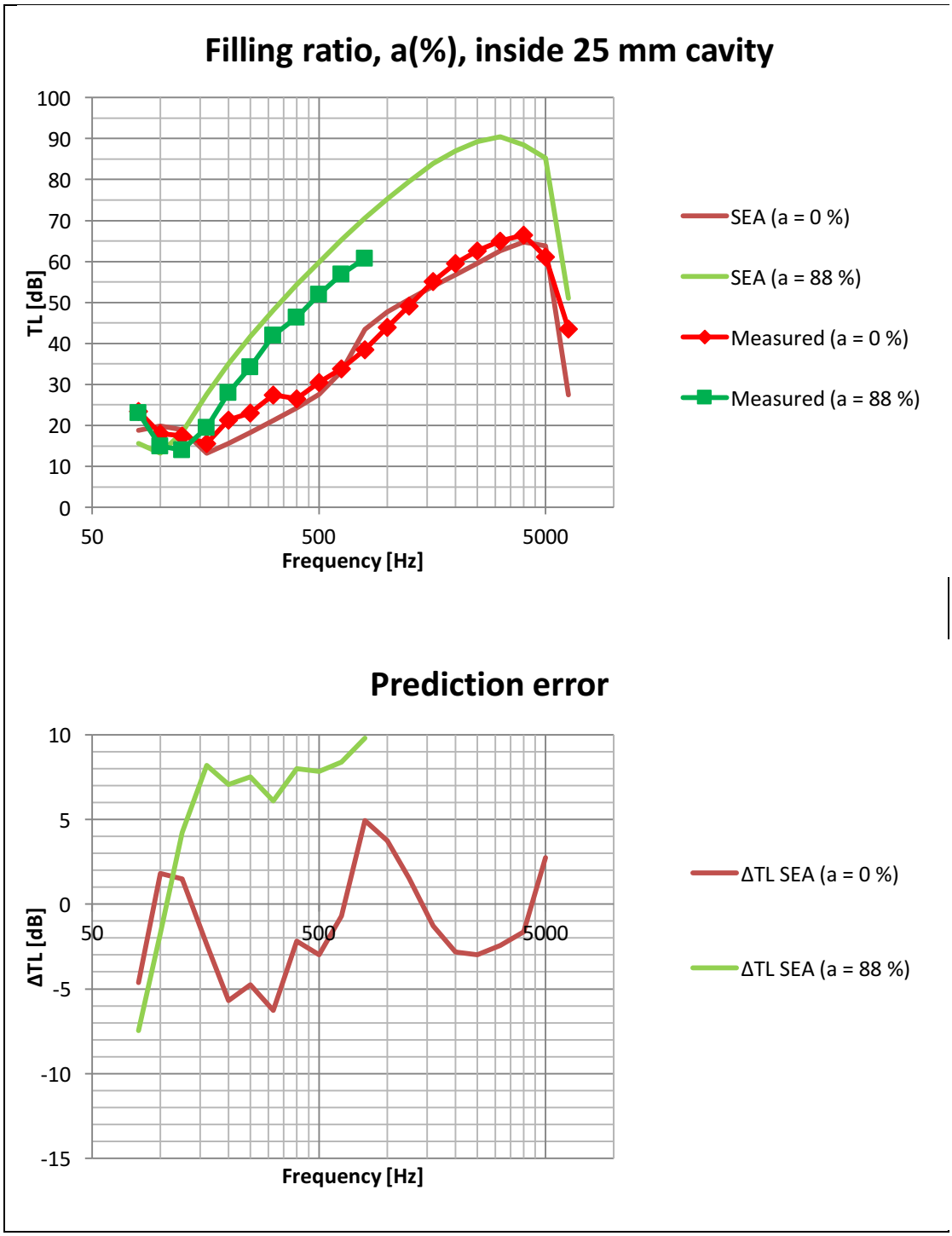

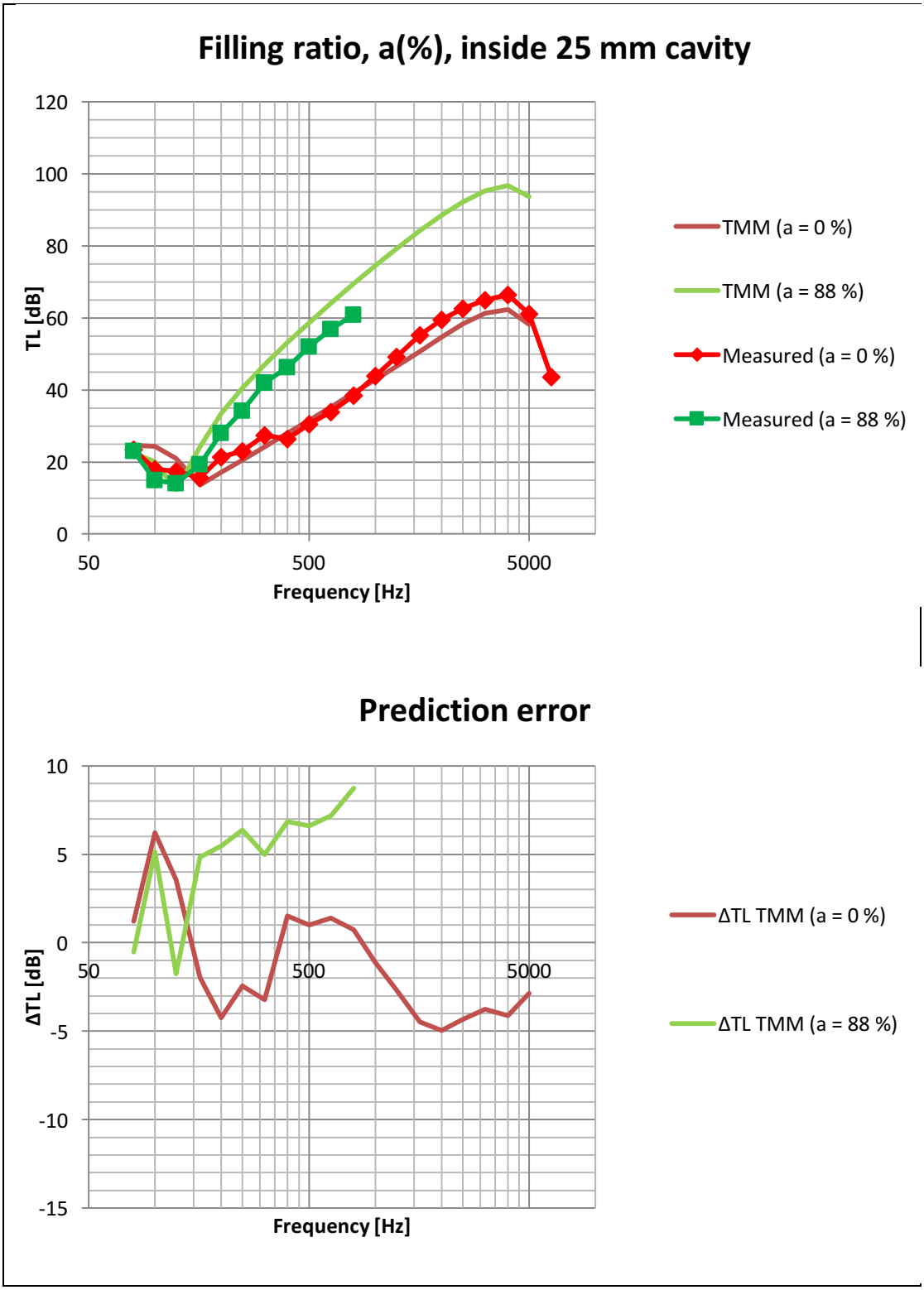
Filling ratio, a(%), inside 25 mm cavity
120
100
80
60
40
20
0
TL [dB]
50
500
5000
Frequency [Hz]
TMM (a = 0 %)
TMM (a = 88 %)
Measured (a = 0 %)
Measured (a = 88 %)
Prediction error
10
5
0
-5
-10
-15
ΔTL [dB]
50
500
5000
Frequency [Hz]
ΔTL TMM (a = 0 %)
ΔTL TMM (a = 88 %)